Diogo Telmo Relvas Figueiredo

Characterization of Carbon Nanotubes dispersions for application in soil stabilization

Master's thesis in the scientific area of Chemical Engineering, supervised by *Professor Doctor Maria da Graça Bomtempo Vaz Rasteiro* and *Professor Doctor António Alberto Santos Correia* and submitted to the Department of Chemical Engineering, Faculty of Science and Technology, University of Coimbra

March 2014

· U C ·

Universidade de Coimbra

Diogo Telmo Relvas Figueiredo

Characterization of carbon nanotubes dispersions for application in soil stabilization

Master's thesis in the scientific area of Chemical Engineering, submitted to the Department of Chemical Engineering, Faculty of Science and Technology, University of Coimbra

Supervisors:

Professor Doctor Maria da Graça Bomtempo Vaz Rasteiro

Professor Doctor António Alberto Santos Correia

Institutions:

Department of Chemical Engineering, Faculty of Science and Technology, University of Coimbra

Department of Civil Engineering, Faculty of Science and Technology, University of Coimbra

Coimbra, 2014

Acknowledgements

My academic career came to an end with the completion of this work. I take this small space to leave few but heartfelt words addressed to all persons and institutions that, deep down, were the lines of the railway which was my course and this work was the last station. Therefore, I thank:

Professor Doctor Maria da Graça Rasteiro for accepting to be my supervisor in this work and having given me certainty that I would have all the materials available whenever needed, for sharing knowledge, for the rigor that she showed me, the suggestions and willingness to answer my questions;

Professor Doctor António Alberto Santos Correia for accepting to be my co-supervisor, for integrating me in the geotechnical laboratory, for the patience in explaining me countless times basic concepts of Civil Engineering, for the suggestions and willingness to answer my questions;

Professor Maria da Graça Castro, for the availability to analyze and correct the spelling and helping me develop my English;

Mr. José António, technician at the *Laboratório de Geotecnia* that, with all his experience, was able to detect and correct errors in the preparation and carrying out of the laboratorial tests and by the company until post-labor times;

AQUATECH, in the person of *Doctor David Hunkeler* for supplying the surfactants, to *Cimpor*, in the person of *Eng. Paulo Rocha* and *Eng. Teresa Martins*, for supplying the binder (Portland cement) and to *Instituto Pedro Nunes* for lending the ultrasound probe;

All my friends that supported me either in good or bad moments, namely *Marta*, *Patrícia*, *Tiago, Luis* and *João* for the study hours and cooperation in this work and in many other group works;

And because the latter are always first, I cannot forget all my family, namely my parents, sister and grandparents, to whom I dedicate this work, for the force that they gave me, for the great effort that they have made to turn this journey possible and for making me who I am today.

To all, that one way or another have given their support, thank you very much!

Abstract

The discovery of the unique properties of carbon nanotubes did grow interest to its application in nanocomposites, for a wide variety of purposes and, nowadays, the amount of applications in which they are used is unimaginable. However, the greatest challenge for its application is associated with the natural tendency to aggregate, resulting in the loss of its beneficial properties. To overcome this problem it is common the use of surfactants (anphiphilic polymers) and/or ultrasonic energy to promote dispersion of carbon nanotubes in suspension.

This work is focused on the application of carbon nanotubes on soil stabilization and on the study the influence of the quality of dispersions on the behavior of soil.

For this, four surfactants (Glycerox, Amber 4001, Disperse 31 and Disperse 32) were characterized followed by the study of which surfactant concentrations were more efficient on the dispersion of carbon nanotubes. The characterizations relied on light scattering techniques, including Dynamic and Static Light Scattering. It was found that only two surfactants had the ability to disperse carbon nanotubes: Glycerox and Amber 4001. The dispersions of carbon nanotubes in these two surfactants were then fully characterized.

Finally, the dispersions of carbon nanotubes have been added to the main agent responsible for soil stabilization, the binder, and the behavior of soils was studied by unconfined compressive strength tests.

The results of unconfined compressive strength tests led to conclude that the introduction and, especially, the quality of the dispersions of carbon nanotubes have huge impact on the mechanical properties of soil. It is verified an improvement up to 77% in compressive strength and 155% in Young's modulus, referred to the reference test where no carbon nanotubes were added, fundamentally dependent on surfactant type and concentration applied.

Keywords: Nanocomposites; Carbon nanotubes; Dispersions; Surfactants; Characterization; Soil.

Resumo

A descoberta das propriedades únicas dos nanotubos de carbono fez despontar o interesse da sua aplicação em nanocompósitos para diversas aplicações e, actualmente, a quantidade de aplicações em que são usados são já imensas. No entanto, o maior desafio para a sua aplicação está associado à tendência natural que têm para agregar, resultando na perda de grande parte dos benefícios associados. Para se contornar este problema é comum recorrer-se a surfactantes (polímeros anfifílicos) e/ou energia ultra-sónica para promover a dispersão dos nanotubos de carbono em suspensão.

Neste trabalho pretende-se estudar a possibilidade de aplicar nanotubos de carbono na estabilização de solos e estudar-se a influência da qualidade das dispersões no comportamento mecânico do solo. Para isso, caracterizam-se quatro surfactantes (Glycerox, Amber 4001, Disperse 31 e Disperse 32) e determinou-se quais as concentrações de surfactante que tornam mais eficientes as dispersões dos nanotubos de carbono. As caracterizações foram feitas com base em técnicas de dispersão da luz, nomeadamente Dynamic e Static Light Scattering. Do estudo realizado, verificou-se que apenas dois surfactantes tinham capacidade de dispersar os nanotubos de carbono: Glycerox e Amber 4001.

Por fim, as dispersões de nanotubos de carbono foram adicionadas ao principal agente responsável pela estabilização de solos, o ligante, e o comportamento dos solos foi estudado através de ensaios de compressão simples.

Os resultados dos ensaios de compressão simples, permitem concluir que a introdução e, especialmente, a qualidade das dispersões de nanotubos de carbono têm grande impacto nas propriedades mecânicas do solo. Verificam-se ganhos até 77% em resistência à compressão simples e até 155% no módulo de elasticidade, dependentes, fundamentalmente, do tipo e concentração do surfactante utilizado.

Palavras-chave: Nanocompósitos; Nanotubos de carbono; Dispersões; Surfactantes; Caracterização; Solo.

Index

Figures Index

Tables Index

Nomenclature and Symbols

Nomenclature/Acronyms

CEM I 42.5 R	Portland cement type I with chemical resistance 42.5
CMC	Critical micelle concentration
CNF	Carbon nanofibers
CNT	Carbon nanotubes
CP	Cement paste
DLS	Dynamic light scattering
FCTUC	*Faculdade de Ciências e Tecnologia da Universidade de Coimbra*
MW	Molecular weight
MWCNT	Multi-wall carbon nanotubes
PCS	Photon correlation spectroscopy
PVC	Polyvinyl chloride
QELS	Quasi-elastic light scattering
SEM	Scanning electron microscope
SFC	Surfactant
SLS	Static light scattering
SWCNT	Single-wall carbon nanotubes
UCS	Unconfined compressive strength
ZSN	ZetaSizer Nano ZS

Symbols

A	Cross-sectional area of the sample
A_c	Corrected cross-sectional area of the sample
^{av}	Averaged values
Al_2O_3	Aluminium oxide
A_2	Second Virial coefficient
C	Concentration
CaO	Calcium oxide
D	Diameter of the sample
D_c	Diffusion coefficient
D_h	Hydrodynamic diameter
D_i	Hydrodynamic diameter of the class i

dn/dc	Differential refractive index increment
D_z	Intensity weighted harmonic mean size of the hydrodynamic diameter distribution
E_{u50}	Secant undrained Young's modulus
ε	Vertical strain
F	Force
Fe_2O_3	Iron oxide
h	Height of sample
I_A	Residual scattering intensity of the analyte
I_i	Scattered light intensity of class i
I_T	Toluene scattering intensity
k	Boltzman's constant
K	Optical constant
MgO	Magnesium oxide
n_o	Solvent refractive index
N_A	Avogadro's constant
n_T	Toluene refractive index
P_θ	Angular dependence of the sample scattering intensity
q_u	Compressive strength obtained
$q_{u\ max}$	Maximum compressive strength obtained
R_θ	Rayleigh's ratio
RI	Refractive index
R_T	Rayleigh's ratio of toluene
SiO_2	Silicon dioxide
SO_3	Sulfur trioxide
T	Thermodynamic temperature
μ	Dynamic viscosity
var	Variation of values from the reference value.
W_f	Final water content
$\Delta\delta_v$	Variation of the axial deformation
λ_o	Laser wavelength

1 Introduction

The sudden growth of urban areas based on good quality soils made arise the need of construction in soils with low geotechnical characteristics, characterized by low resistance and high deformability.

These soil characteristics require special care in order to make possible the construction on such soils and the adoption of reinforcement or stabilization techniques are common, including the chemical stabilization of soil, the subject of study of this work. Chemical stabilization of a soil is not more than the aggregate of soil particles by introducing materials with binder properties, endowing the new material with better mechanical characteristics (higher strength and lower deformability than the original soil).

Traditionally, a suspension/syrup with Portland cement was added to stabilize chemically the soil. However, given the structural requirements, it is necessary to develop techniques that improve further the performance of cement stabilization of soils, in particular to increase their mechanical strength.

The aim of this work is the use of carbon nanotubes (CNT) to improve the efficiency of soil stabilization.

The CNT were discovered recently, in the early 90's, however, the research involving the properties and applications of this material is numerous and in many areas.

The unique mechanical and electrical properties make the CNT great tools in the area of nanotechnology. So the incorporation in composites of polymers or other materials can be quite advantageous, improving certain properties and/or the performance of the material.

The incorporation of this type of nanosized particles in cement matrices allows them to acquire improved properties, increasing the performance of soil stabilization. However, the direct application of the CNT in cement is not possible, due to the natural tendency of aggregation of these nanosized particles into larger aggregates, which causes the loss of the beneficial effects associated with their incorporation.

Thus, an important step of the incorporation of CNT in cement matrices is its stabilization/dispersion on the suspension that will be added to the soil. For this purpose, mechanical (ultrasounds) and chemical (surfactants) strategies are used.

The use of ultrasounds should be minimized because it is an energy-inefficient technique, thus the use of surfactants can help in minimizing ultrasounds requirement. The better the dispersion of CNT within a specific surfactant, the smaller will be the amount of ultrasonic energy required for application in the same suspension.

The plan for the implementation of this new strategy starts with the characterization of four different surfactants supplied by *AQUATECH, Switzerland*. The four surfactants are Glycerox, Amber 4001, Disperse31, and Disperse32. Then the dispersions of CNT for various concentrations of surfactant were characterized, to determine the best concentration to be used in the soil. Finally unconfined compressive strength tests (UCS) were performed for the various samples of stabilized soil, varying the CNT and surfactant concentration for each surfactant studied. The higher the values of compressive strength and Young's modulus, the better is the soil stabilization.

This work is divided in five chapters:

- Chapter 1 is the introduction, where the problem is described and the objectives are exposed;
- Chapter 2 is the state of art where the global fundaments and similar works and conclusions presented by other authors are exposed;
- Chapter 3 is the materials and procedures characterization where the CNT, surfactants, binder, soil, detailed experimental procedures, techniques employed and test plan are described;
- Chapter 4 is where the results of the characterization of the dispersions and UCS tests are presented and discussed;
- Chapter 5 is the conclusion and future works where the principal conclusions are listed and complementary works are proposed.

2 State of the Art

2.1 Carbon nanotubes

2.1.1 Background

The year of 1991 was in course when Sumio Iijima, Japanese physicist and researcher at NEC Corporation, published some observations in a transmission electron microscope of a kind of micro tubes whose walls were formed by carbon atoms linked in hexagonal form, long and with between 2 and 20 concentric layers, forming a tubular structure. The smaller tube featured a 2.2 nm diameter that corresponds approximately to a ring of 30 hexagons of carbon [1]. For better understanding, this tubular structure can be compared with a strand of hair but at the nanoscale. It was precisely due to the nanosized diameter that Sumio Iijima gave them the name of carbon nanotubes (CNT). The unique features of this structure could allow unimaginable applications and made to believe that it was a material that could revolutionize the future. This work did dawn several researches about this new chemical structure and currently there are many applications of CNT and many more are under intense study. According to Figure 1, the anual progress between 1992 and 2010 in CNT publications increased exponentialy, in average 10% each year, proving the increased interest about this theme [2].

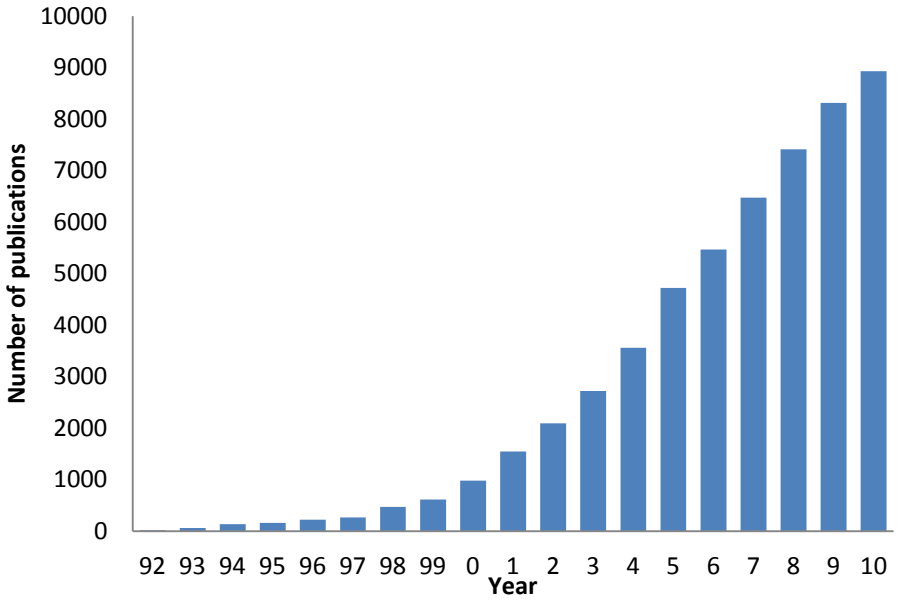

Figure 1 - Evolution of number of publications about carbon nanotubes [data from 2].

Due to its valence, the carbon can easily establish links with other elements. Depending on how the atoms arrange themselves, it is capable of forming very fragile structures like the graffiti and very rigid structures such as diamond and others such as the new family of spheroidal or cylindrical molecules like fullerenes or CNT respectively. These various settings are called allotropes. The graphite is a network consisting of several overlapping layers of carbon atoms linked in hexagonal form. On the other hand, graphene is just one of these planar layers. A carbon nanotube is one of these sheets of graphene, wrapped, forming a hollow tube. There are many ways to roll this sheet into a cylinder resulting in different diameters and microscopic structures resulting in different properties.

2.1.2 Classification of CNT

The CNT can be classified as being of multiple-wall (MWCNT) or single-wall (SWCNT). MWCNT consists of a series of two or more tubes coiled around each other concentrically, forming a wall with the thickness of more than one carbon atom and capped at end as firstly reported by Iijima in 1991 (Figure 2) [3]. SWCNT only consists of one of these tubes, with only one dimension, i.e. with the thickness of just 1 atom and was firstly reported two years later, in 1993 [4,5]. The way the graphene sheet is wrapped sets the final structure and in Figure 3 three different structures are represented: armchair (A), chiral (B) and zig-zag (C) [6]. MWCNT are less expensive, more readily available and have chemical resistance substantially greater than SWCNT [7]. While the SWCNT have diameters typically on the order of 0.4-3nm, MWCNT may have diameters of 1.4 until at least 100nm, so the diameter is an important variable in the definition of the properties of the CNT [7]. Although smaller size and massive arrangement in ropes are distinctive characteristics, it makes the measurement of the mechanical properties of SWCNT more complex and less precise [8].

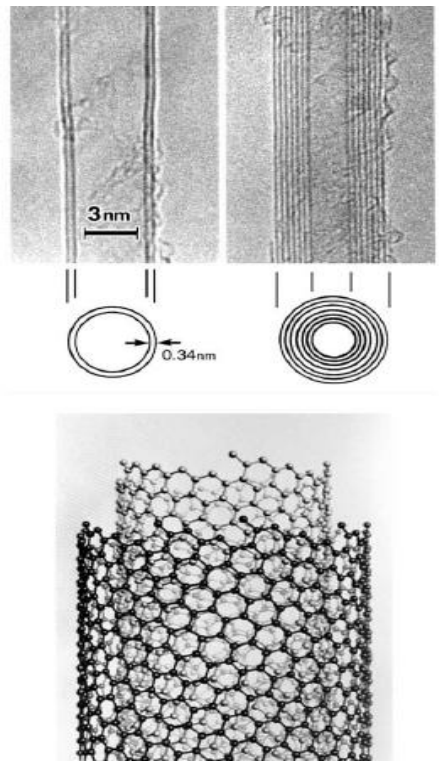

Figure 2 - MWCNT discovered by Iijima in 1991 [3].

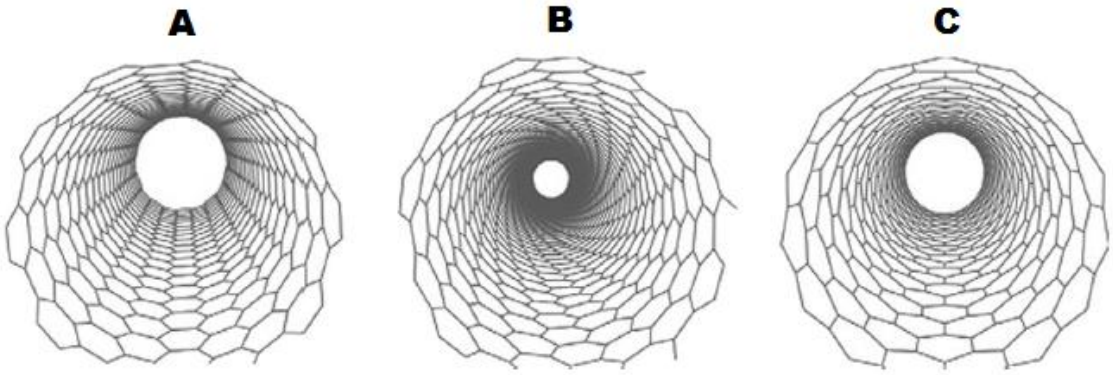

Figure 3 - Structures of SWCNT. Armchair (A), chiral (B) and zig-zag (C) [6].

2.1.3 Properties of CNT

Chemical properties

Carbon atoms in CNT form bonds in the hexagonal sp^2 hybridization state. Consequently these atoms have strong non-polar covalent bonds and a hydrophobic surface making them difficult to disperse in solution. Such surface interactions combined with Van de Waals forces and the high aspect ratio of CNT, results in their agglomeration [9].

As referred in section 2.1.2, chemical resistance is one important factor that favors the MWCNT. The several layers of MWCNT favors surface functionalization, possible because only the outer wall is modified. In the case of SWCNT, covalent functionalization will break some carbon-carbon double bonds, leaving holes in the structure of the nanotube and, thus, changing negatively its mechanical properties [10].

Physical properties

The CNT are one of the nanometric materials of greatest potential to reinforce materials matrices because exhibit resistance with exceptionally high Young's modulus in order of TPa and resisting stress in order of GPa, approximately 5 and 100 times higher than steel, respectively. The density is less than 1800 kg/m^3, about one-sixth than steel, and feature an interesting aspect ratio (length /diameter) of 1000 or higher [11].

Electrical properties

CNT can display either metallic or semiconducting electronic properties due to the topological defects from the fullerene-like end caps in CNT. Thus, the CNT electrical properties are dependent upon their dimensions, helicity or chirality [11]. Some methods were

developed to obtain specific electronic properties that favor the use of post-processing such as ultra-high speed centrifugation. For the above reasons (CNT can display either metallic or semiconducting electronic properties), any sample of CNT typically displays a wide range of electronic properties, even though the CNT may superficially appear the same in length, diameter or otherwise [9].

2.2 Formation of nanocomposites

Initially, blending of different class of polymer was used to fabricate new materials with unique properties. However, blending lead to only minimal improvement in physical properties which were still inadequate for engineering applications. So to improve the strength and stiffness of polymer materials, different kinds of organic and inorganic fillers were used. However, processing these materials is very difficult, therefore small fiber or particle reinforced composites were developed. The common particle fillers used were silica, carbon black, metal particles, etc. But significantly high filler loading was required to achieve desired mechanical property, which thus increased cost and made processability difficult. So to achieve high mechanical properties at lower filler loading, nanofillers were used. The nanofiller reinforced polymer matrix is known as polymer nanocomposite [12].

From the knowledge acquired till now, it is possible to enter the field of the so-called nanoengineering that encompasses the techniques of manipulation of nanometer-level structures in order to develop composites, specifically designed and multifunctional with mechanical properties and potential durability rather superiors [13].

Incorporation of CNT in polymer matrices provides materials that could be used for many high performance engineering applications. Currently, the most widespread use of CNT nanocomposites is in electronics. These nanocomposites could be used to shield electromagnetic interference and as electrostatic-discharge components [14]. The CNT are promising candidates for the adsorption of heavy metals to reduce environmental problems like removal of heavy metals from wastewaters [15]. The microwave-absorbing capability of CNT may have applications in space exploration [16]. CNT are helpful in preparation of silicone-based coatings with application as marine fouling release coatings [17]. Catalyst supporter [18, 19] and chemical sensors [20, 21] are other areas where CNT are widely applied.

The cement can be embedded by nanoparticles as the CNT control the behavior of materials or to add new properties which result in better performances.

The methodologies that allow introduce new molecules in the cement structures may occur in several phases: solid, liquid or liquid-solid interface or solid-solid interfaces. Although it is recognized that nanoengineering has great potential, some challenges still remain, in particular, the ease of obtaining dispersions suitable at the nanoscale dimension, scale-up and reduction of the cost/benefit ratio.

Nanosized particles have high surface/volume ratio which allow them to have great capacity to react chemically. However, it is necessary to ensure good dispersion, avoiding particles agglomeration because the aggregates decrease the specific surface and thus decrease the benefits associated with their size. Thus, a pre-requisite for the successful use of CNT properties in a composite structure is the effective utilization of their high aspect ratio, for which their disaggregation and preferential alignment are essential. The great difficulty relating to the quality of dispersion is due mainly to its hydrophobic characteristics and its strong and natural tendency towards aggregation. Bad CNT dispersions lead to the formation of defective sites in nanocomposites and limit the efficiency of the CNT in the cement matrix.

Konsta-Gdoutos et al. [22] studied a cement matrix with highly dispersed MWCNT. To disperse the MWCNT homogeneously in the mixing water, MWCNT suspensions were prepared by adding the MWCNT in an aqueous surfactant solution. The resulting dispersions were sonicated at room temperature following the method described in [23-25]. Two types of MWCNT were used, long and short ones, all with the same diameter. The MWCNT were added to an aqueous solution enriched with a surfactant with the following concentrations of MWCNT: 0.048%, 0.08% and 0.1% (short) and 0.025%, 0.048% and 0.08% (long) by weight. The suspension of MWCNT with a ratio of MWCNT/surfactant equal to 4 by weight was added to Portland cement paste with a water/cement ratio of 0.3 by weight.

Figure 4 shows scanning electron microscope (SEM) images under above conditions, used to evaluate the dispersion of MWCNT. When dispersion is not good there are large agglomerates of MWCNT (A) and good dispersion corresponds to the existence of individual MWCNT (B).

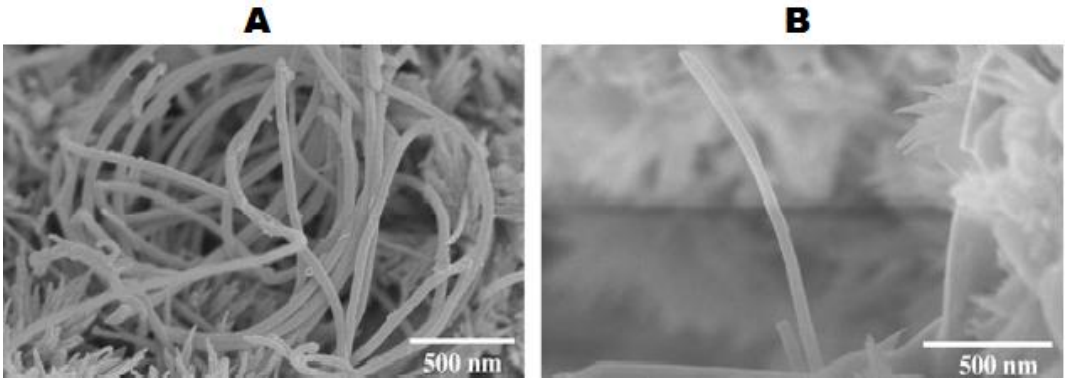

Figure 4 - SEM images of cement paste fractures with undispersed (A) and dispersed (B) MWCNT [22].

There are two distinct approaches for dispersing CNT: the chemical and mechanical methods. These two methods are often utilized simultaneously. Both are described below.

2.2.1 Chemical method

This method is designed to alter the surface energy of the solids and can be classified as covalent or non-covalent.

CNT are often entangled and they have high tendency to rapidly re-aggregate if no special treatment or surface agent is used to maintain them in a dispersed state.

The chemical interactions of CNT can be modified through the addition of functional groups which establish covalent bounds with CNT. This is called functionalization and usually includes the addition of carboxyl or alcohol groups which are normally used to assist the dispersion of CNT in water [9]. The strength of CNT is directly dependent on the number of lattice defects. Although defect-free CNT are desirable in maximizing many properties, they can hinder bonding within the cement matrix. Defect-free CNT will simply pull out of cement with minimal effort. Lattice defect sites on CNT provide a location for the formation of those bonds. It improves their chemical compatibility with the target medium (solvent or polymer solution), that allow enhance wetting or adhesion characteristics and reduce their tendency to agglomerate. However, aggressive chemical functionalization, such as the use of neat acids at high temperatures, might introduce structural defects resulting in inferior properties for the CNT [8].

Typical acid functionalization uses two highly concentrated acids; nitric acid (HNO_3), which oxidizes the surface, and sulfuric acid (H_2SO_4), which roughens the surface. When a surface is roughened the carbon-carbon bonds are broken, creating defect sites. This allows the nitric acid to create functional groups on the surfaces of nanofilaments. However, the

rougher the surface, the weaker the nanofilaments. Another negative side effect of sulfuric acid is its ability to diffuse through sections of nanofilaments. This cuts the nanofilaments into smaller lengths, reducing their aspect ratios [26].

Non-covalent treatment is particularly attractive because of the possibility of adsorbing various groups on CNT surface without disturbing the π system of the graphene sheets. In the last few years, the non-covalent surface treatment by adding surfactants or polymers has been widely used in the preparation of both aqueous and organic solutions to obtain high weight fraction of individually dispersed CNT [8].

The surfactants are polymers that have the ability to accumulate on surfaces or interfaces promoting solids or liquids dispersions in various media. They are of amphiphilic character in nature, which allows them to adsorb at interface between immiscible phases such as oil and water or particles and liquid, reducing surface tension. Surfactants can be classified according to the charge of the hydrophilic region as cationic, anionic and non-ionic. In this way, the driving-force for surfactants adsorption on charged surfaces are the Coulomb attraction between the hydrophilic area of surfactant and solid surface which should have opposite charge. In the case of non-ionic surfactants, they adhere to hydrophobic surfaces through their tails due to Van der Waals forces. After the connection between surfactant and particle surface, the natural tendency of surfactants is to start aggregation in micelles till the critical micelle concentration (CMC). CMC is the concentration above which makes the surfactant adsorb to the particle surface and begins to form micelles.

It became obvious that the properties of certain materials, particularly cement can be improved with the introduction of CNT, which leads to the reduction of the particle spacing in the nanocomposite, as long as dispersion is guaranteed.

Konsta-Gdoutos et al. [27] investigated the surfactant concentration effect on the dispersion of the MWCNT with fracture mechanic tests. Samples were produced with surfactant at different weight ratios and long MWCNT. In Figure 5 is observed that samples treated with different amounts of surfactant exhibit higher fracture load than the sample with no surfactant. The samples with a surfactant/MWCNT ratio of 4 give a higher average load increase at all ages. The authors conclude that surfactant/MWCNT ratios either lower or higher than 4.0 produce specimens with less load increase. The authors explained that at lower surfactant/MWCNT ratio, less surfactant molecules are adsorbed to the carbon surface and the protection from agglomeration is reduced. At higher surfactant/MWCNT ratios, bridging flocculation can occur between the surfactant molecules. Too large amount of surfactant in the aqueous solution is causing the reduction of the electrostatic repulsion forces

between the MWCNT producing again aggregates. The results indicate that for effective dispersion, there exists an optimum weight ratio of surfactant/MWCNT close to 4 by weight.

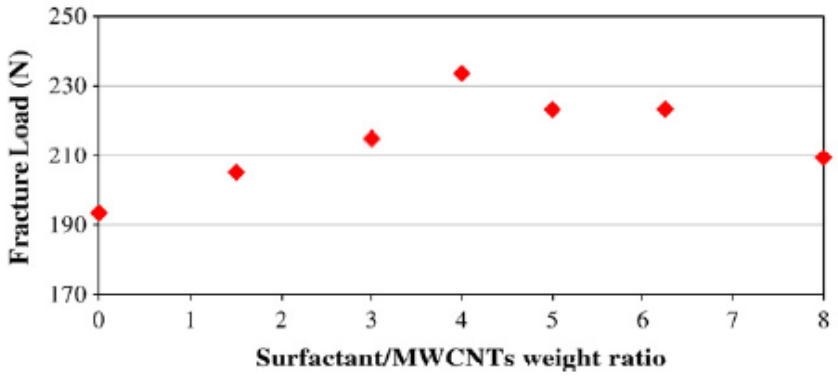

Figure 5 - Fracture load from flexural tests of 28 days cement paste reinforced with long MWCNT [27].

Moore et al. [28] studied dispersions of individual SWCNT in aqueous media using various anionic, cationic and nonionic surfactants. It was determined that polymers with higher molecular weights were able to facilitate the dispersion of higher amounts of CNT. It is explained by the authors, that higher molecular weights enable suspending more CNT due mostly to the size of the hydrophilic group, because of enhanced steric stabilization coming from longer polymeric groups. This type of stabilization is not seen in the ionic surfactants because charge repulsion is the dominating factor impeding aggregation of CNT.

Abu Al-Rub et al. [26] studied the effects of untreated and acid-treated (functionalized) CNT and carbon nanofibers (CNF) on mechanical properties of cement composites, calling them nanofilaments. Both were added to cement paste in concentrations of 0.1% and 0.2% by weight of cement. Each specimen was tested in a custom-made three-point flexural test fixture to record the mechanical properties (Young's modulus, flexural strength, ductility and modulus of toughness) at the age of 7, 14 and 28 days. It was verified that the behavior of composite materials varies significantly along the age. The results clearly showed a drop in mechanical properties when acid-treated nanofilaments are compared with untreated nanofilaments. The following data were noted with the cement paste reinforced with untreated fibers, when compared with the plain cement (reference) at 28 days: the average ductility increased up to 73%, the average flexural strength increased up to 60%, the average Young's modulus increased up to 25%, and the average modulus of toughness increased up to 170%. The authors conclude that these enhancements indicate the presence of interfacial bonds between the nanofilaments and cement, which improved the mechanical properties of the cement paste. However, these enhancements were observed only for untreated

nanofilaments. In general, acid-treated nanofilaments had weaker mechanical properties. This degradation in mechanical properties is attributed to the excessive formation of ettringite [1] caused by the presence of sulfates.

The 0.2% concentration of nanofilaments was considered excessive for cement paste with high aspect-ratio nanofilaments. Therefore, the authors recommended that a nanofilament concentration around 0.1% by weight is a reasonable value for achieving a better dispersion for nanofilaments with regarding high aspect ratios.

2.2.2 Mechanical method

The chemical method of MWCNT dispersions with the use of surfactant, in many cases do not becomes fully effective, so there is the need to resort to mechanical methods, such as ultrasonic energy to ensure even better dispersion. Ultrasonic processors convert voltage to mechanical vibrations. These mechanical vibrations are transferred into the liquid by the probe creating pressure waves. This action causes the formation and collapse of microscopic bubbles. This phenomenon creates millions of shock waves, increasing the temperature in the suspension. Although the amount of energy released by each individual bubble is small, the cumulative effect causes extremely highs levels of energy to be released, resulting in the dispersion of objects and surfaces in the continuous medium.

However, the aim is to use as little as possible of this energy because further it be energy-inefficient, there is also a risk of fragmentation of the CNT, which would lead to a decrease in the aspect ratio, changing its properties. With increasing ultrasonication times MWCNT get shorter and thinner, and ultimately transform into amorphous carbon.

In a typical dispersion procedure, covalent or non-covalent, is often followed by ultrasonication. In the first case ultrasonication, apart from successfully dispersing CNT, has proven to be highly effective in increasing the formation of defect sites for the attachment of functional groups. Thus, various functional groups can covalently attach to these locations providing active nucleation sites for high-loading of nanoparticles [29]. In the second case, after the surfactant has been adsorbed on the CNT surface, ultrasonication for minutes or hours, according to the power of ultrasonic tip, may help a surfactant to separate CNT by steric or electrostatic repulsions.

Konsta-Gdoutos et al. [27] studied the effect of ultrasonic energy on the dispersion quality of CNT suspensions, measuring the rheological properties of cement paste samples

[1] Hydrous calcium aluminium sulfate mineral ($Ca_6Al_2(SO_4)_3(OH)_{12}\cdot 26H_2O$)

reinforced with MWCNT under steady shear stress. Under low shear stress, CNT agglomerates control the viscosity of the suspensions. Therefore, suspensions with larger scale agglomerates exhibit higher viscosity.

Figure 6 shows the behavior of two cementitious nanocomposites reinforced with MWCNT, with and without ultrasonication and compares them to the reference cement paste (CP) and the same amount of surfactant (SFC), but without MWCNT reinforcement. At low shear stress, dispersions without ultrasonication exhibit high viscosity (0.13 Pa.s) while the ultrasonicated dispersions exhibit lower viscosity (0.09 Pa.s) which is very close to the viscosity of the reference paste (0.007 Pa.s). The authors conclude that, as expected, at low stress conditions, the application of ultrasonic energy controls the dispersion of MWCNT. Under high shear stress (>70 Pa) the agglomerates can be broken down by the fluid motions so the viscosities of all suspensions are similar. Based on those results, the authors concluded that for proper dispersion, the application of ultrasonic energy is required.

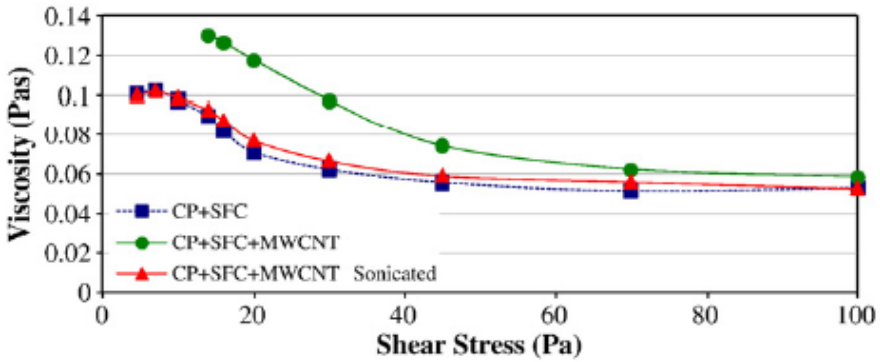

Figure 6 - Variation of viscosity of cement paste, reinforced with long MWCNT, with Shear Stress [27].

A detailed study on the effects of MWCNT concentration and aspect ratio was conducted as described in section 2.2 [22]. In Figure 7 are represented the effect of adding short (A) and long (B) MWCNT in different concentrations on the flexural strength of cement. In all cases, the MWCNT reinforcement shows better results in flexural strength tests regarding to reference cement paste. The intermediate suspensions, both concentrations of 0.08% for small and 0.048% for long MWCNT, showed the best performances. The authors conclude that the dispersions with higher concentrations of MWCNT may be difficult, diminishing the positive effect of the presence of MWCNT in cement. There is therefore an optimum concentration of MWCNT. It is also concluded that less quantity of long MWCNT is needed to reach the optimum concentration, comparing to short MWCNT.

Nevertheless, optimum concentrations of short MWCNT reach higher values of flexural strength than the long ones.

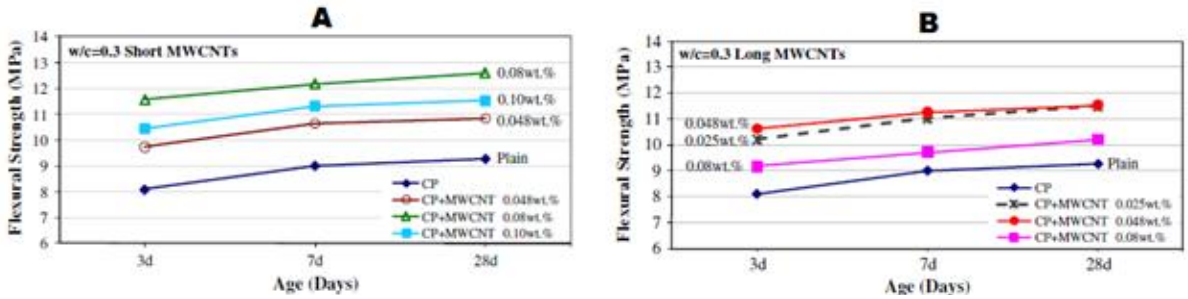

Figure 7 - Effect of short (A) and long (B) MWCNT with a different concentration on the flexural strength of cement [22].

Lestari et al. [30] studied the effect of different dispersants in compressive strength of carbon fiber cementitious composites at curing time of 3, 7 and 28 days. Figure 8 describes how it works. The sample is placed under the press which applies a vertical load on the sample. The behavior of the sample under the applied load is registered in the computer.

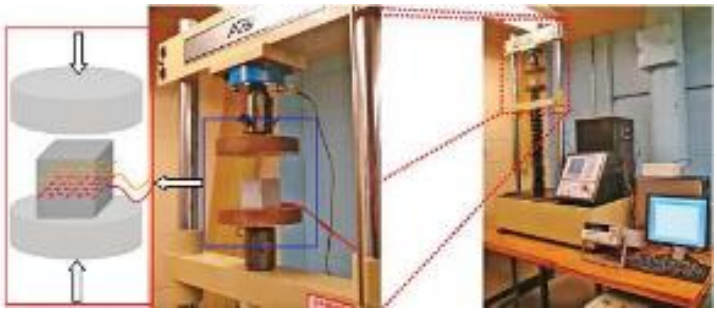

Figure 8 - Compressive strength test [30].

2.3 Chemical stabilization of soil

Chemical stabilization of soil arises in the context of the need to use weak geotechnical soils for the construction. The current practice is to modify the engineering properties of the native problematic soils to meet the design requirements. It is linked with the changes in the chemical composition of the soil matrix. This can be achieved by the mix of soil with cementitious materials such as, polymers of resins, by adding enzymes, by adding cement or other binders to the soil, or by changing the ionic or charge composition of the soil.

The result of this mix are physicochemical interactions that occur between soil particles, the binders and water present in the soil, resulting in a new composite material with a different mechanical behavior of the original one.

In the presence of organic soils and/or when it wishes to confer high mechanical resistance to the stabilized material, it is common to refer to the Portland cement as main cementitious material [31]. Portland cement modifies and improves the quality of soil for the purpose of increasing strength, stiffness and durability. The amount of cement used will dictate whether modification or stabilization has occurred.

To meet the characteristics of the soil, such as the existence of organic matter, very high water content and soil heterogeneity in depth, it is usual to the addition of additives to the main binder, with the environmental advantages arising from the fact that, in some cases, to reuse industrial by-products. Per example, Li Chen and Deng-Fong Lin [32] mixed sewage sludge with cement for use as stabilizer to improve the strength of soft subgrade soil. Yang et al. [33] showed that silica and calcite were observed in dry sewage sludge crystallization using DRX analysis. Therefore, the addition of sewage sludge ash to mortar could slow hydration processes of the cement. Furthermore, Lin et al. [34] applied nano-SiO_2 as an additive to improve the properties of sludge ash tiles. The authors showed that the flexural strength of sludge ash tiles increased with the increasing amounts of nano-SiO_2. Hurley and Thornburn [35] studied the effect of sodium silicate on the stabilization of lime and cement, and found that sodium silicate helps improve soil strength. Silica fume is another cement replacement mineral additive that has been used for producing high-performance concrete [36].

The aim of present work is to achieve appropriate CNT dispersions, used as additive to Portland cement matrix in order to improve the mechanical behavior of soft soils of low Mondego River. This specific application was not found in the literature.

3 Characterization of materials and experimental procedures

3.1 Overview

This chapter refers to the characterization of the materials used, as well as of the procedures adopted to achieve the objective of the present study: characterization of CNT dispersions for application in soil stabilization. The tests that will be carried out were conducted on samples prepared in the laboratory, since their preparation obeyed certain criteria in order to ensure, to the extent possible, the homogeneity and reproducibility of the samples as well as reproduction of field conditions.

Based on information gathered in the previous chapter, a proper dispersion requires the use of a surfactant and ultrasonic energy. In order to study the best way to disperse the multi-wall carbon nanotubes (MWCNT), various types of surfactants were tested in different concentrations.

Initially, the characterization of the surfactants was performed, in particular, the evaluation of the hydrodynamic diameter and molecular weight. Then, the MWCNT dispersions were characterized for the various concentrations of surfactant, assessing the size of the particles. Finally, unconfined compressive strength (UCS) tests were conducted to evaluate the mechanical performance of a soil chemically stabilized with a binder which incorporates MWCNT properly dispersed in an aqueous solution enriched with a surfactant.

3.2 Materials

3.2.1 Carbon nanotubes

In this study, it was decided to use MWCNT mainly due to cost (100€/kg) which is significantly inferior to the SWCNT. These MWCNT are from the Nanocyl company and according to their data, the MWCNT CN7000 have an averaged diameter of 9.5 nm, averaged length of 1500 nm and a specific surface between 250000 and 300000 m^2/kg. MWCNT are consisted essentially of pure carbon (90%), with some metal oxides (10%) and negative electrical charge (-25, 2 mV). The refractive index of MWCNT was considered equal to the one of carbon in the pure state (2.42) [37].

3.2.2 Surfactants

It was seen in section 2.2.1, that the surfactants are polymers which have the ability to accumulate on surface or interface of the MWCNT, promoting their dispersion in aqueous solutions. In this study four different surfactants were tested in order to assess the best conditions in order to promote the dispersion of the MWCNT. Table 1 lists the information provided by the surfactants' supplier. Concentration values are by weight. The surfactants Disperse 31, Disperse 32 and Amber 4001 were produced and supplied by the company AQUATECH. The Glycerox is a commercial surfactant which is produced by another company (Lubrizol), although it has also been supplied by the same company.

Table 1 - Surfactants used and data provided by the supplier.

Surfactant (-)	**Concentration (%)**	**Charge (-)**	**Chain type (-)**
Glycerox	31	Nonionic	Linear
Amber 4001	50	Cationic	Linear
Disperse 31	25	Anionic	Linear
Disperse 32	35	Anionic	Linear

Further characterization of the surfactants was conducted in order to facilitate the understanding of their performances. Normally, one of the most important properties to characterize is the average hydrodynamic diameter of the molecules. However, most materials are composed of a set of irregular particles with different dimensions. Thus, it is necessary to define equivalent dimensions obtained by measuring a property of the molecule somehow related to its size. From this property, an averaged linear dimension of the particle that characterize the surfactant's molecule conformation was calculated.

Molecular weight plays an important role on the performance of the surfactants, namely when was considered its efficiency on the dispersion of a particulate system.

Varadaraj [38] compared two types of ethoxylates, linear and branched, with the same number of oxyethylene groups. Branched ethoxylates exhibit a higher critical micelle concentration (CMC) and are more effective in reducing the surface tension at the air-water interface by occupying a larger area per molecule. Achouri et al. [39] demonstrate that the presence of two hydrophobic groups in the surfactant molecule results in greater surface activity.

It was decided to measure the size of the molecules and the molecular weight for complete characterization of surfactants. The equipment used was the ZetaSizer Nano ZS (ZSN) by Malvern, installed on *Laboratório de Tecnologia de Sólidos* of Chemical Engineering Department of *Faculdade de Ciências e Tecnologia da Universidade de Coimbra* (FCTUC).

3.2.3 Binder

With the purpose of chemical stabilization of a soil, binders are added and mixed, causing reactions of physicochemical nature with soil particles and with water, which improve the mechanical behavior of the resulting mixture.

The binder mostly used is cement and its mixture with water initiates spontaneously a chemical process known as hydration reactions. The hardening of cement will enclose soil as glue, but it will not change the structure of soil. These reactions occur in two phases: primary hydration, which consists of almost instantaneous reactions, which lead to a significant decrease in water content; the second phase is the secondary hydration, where slower reactions occur with a smaller "consumption" of the water available. In this second phase, the resulting resistance increases as a function of time, i.e. for longer curing times higher strength is obtained.

The Portland cement used is of type I, class of mechanical resistance 42.5 (CEM I 42.5 R) and its composition in terms of the main constituents is given in Table 2. The cement is negatively charged (zeta potential measured was -2.14 mV and it is according to Srinivasan et al. [40]).

Table 2 - Main constituents of Portland cement.

	CaO	**SiO_2**	**Al_2O_3**	**Fe_2O_3**	**MgO**	**SO_3**
Quantity (%)	62.84	19.24	4.93	3.17	2.50	3.35

3.2.4 Soil

The present work is based on the soil collected in an agricultural portion of land located in the *Quinta da Foja* reserves between *Coimbra* and *Figueira da Foz*.

The soil is mostly composed of silt with some clay, sand particles and organic matter. Generally speaking, it is a soft soil with low resistance, permeability and high compressibility,

which is reflected in weak geotechnical characteristics. So, if there is a need to build any structures, difficulties will be expected. The soft soil is characterized by the presence of high amount of organic matter which can hinder the hydration process by retaining the calcium ions. In such soils, successful stabilization depends on the proper selection of binder type and amount of binder added.

The soil studied was collected to a depth of 2.5 m and was transported to the *Laboratório de Geotecnia* of Civil Engineering Department of FCTUC in three boxes of approximately 1 m^3 each, protected by plastic sleeves and plastic wrap to prevent water loss from the soil in the field, where it presents a high value of water content (80.87%). The water content is a parameter that characterizes soft soils because it has direct influence on their natural and stabilized properties. The lower the water content, the higher its mechanical resistance of the soil, but only up to a certain minimum value of humidity. Below this value of humidity, the binder doesn't find the necessary water to react totally. A certain amount of the soil collected was homogenized in the laboratory. The soil was withdrawn randomly from the boxes and was homogenized using a mixer (Hobart N50) before adding up to 57.520 kg of soil in a small box. The water content was measured and was lower than the desired, so some water was added to keep water content around 80.87%. All samples tested were prepared from the soil of this small box.

The procedure used to homogenize the soil aimed to control variations in the main characteristics of the soil, making it easy to have representative samples of the soil in its natural conditions, where organic content is about 10%. Once homogenized, the necessary soil for the accomplishment of this work was packaged in a thermo-hygrometric chamber at a temperature of 20 ± 2° C and a relative humidity of 95 ± 5% until the date of use.

A more detailed description and characterization of the soil can be found in [41].

3.3 Experimental procedure

3.3.1 Characterization techniques

The ZSN is an equipment which has three functions [42]:

- A molecular size analyzer for the enhanced detection of particle aggregates and measurement of molecules of diluted samples, using dynamic light scattering;
- A molecular weight analyzer using static light scattering. Molecular weight measurement range is possible from a few g/mol to 500 for linear polymers and 20000 kg/mol for near spherical polymers and proteins;

- A zeta potential analyzer that uses electrophoretic light scattering for particles, molecules and surfaces.

Size measurement

Dynamic Light Scattering (DLS), also known as Photon Correlation Spectroscopy (PCS) or Quasi-Elastic Light Scattering (QELS), is a non-invasive, well-established technique for measuring the size and size distribution of molecules and particles typically in the submicron region. Typical applications of dynamic light scattering are the characterization of particles and emulsions or molecules, which have been dispersed or dissolved in a liquid [43]. As the particles are constantly in motion, the intensity of light dispersed by the particles appears to fluctuate. The ZSN system measures the rate of intensity fluctuation and then uses this to calculate the size of particles. The signal intensity of the light scattered by a particle decreases with time and ZSN system measures several signals with time scales in order of nanoseconds. The similarity of two intensity signals is called correlation. Two consecutive signals are strongly correlated and two signals separated in time scale will be less correlated till no correlation occurs.

In Figure 9 are represented typical correlation functions for small and large particles. As can be seen, the rate of decay for correlation function is related to particle size. Larger particles move slowly, the intensity signal and the rate of decay fluctuate more slowly than for the smaller ones.

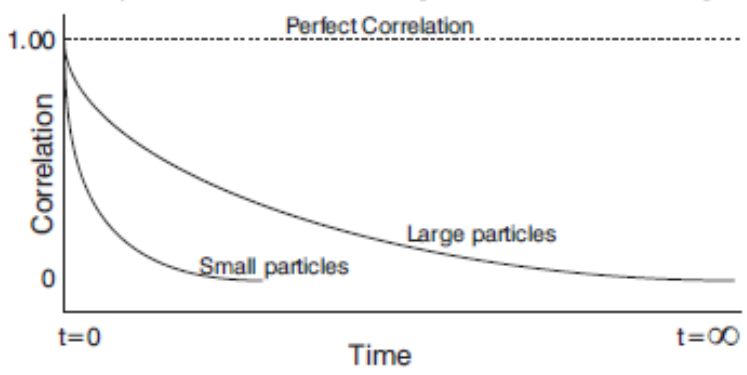

Figure 9 - Typical correlations for small and large particles.

Embodied within the correlation curve is all the information regarding the diffusion of particles in the measured sample. By fitting the correlation curve to an exponential function (cumulants method) or to a sum of exponential functions (CONTIN method, adequate to more complex samples), the distribution of diffusion coefficient (D_c) can be calculated. With

diffusion coefficient distribution, the conversion to a hydrodynamic diameter distribution is possible by using Stokes-Einstein equation (Equation 1). Hydrodynamic diameter (D_h) is the equivalent dimension to characterize the size of particles in a DLS measurement and is defined as the size of a hypothetical hard sphere that diffuses in the same way as that of the particle being measured.

$$D_c = \frac{kT}{3\pi\mu D_h} \quad \text{(Eq. 1)}$$

- D_c is the diffusion coefficient;
- k is Boltzman's constant;
- T is thermodynamic temperature;
- μ is the dynamic viscosity;
- D_h is the hydrodynamic diameter.

D_z (or Z-Average) is the intensity weighted harmonic mean size of the hydrodynamic diameter distribution. The D_z increases as the particle size increases. Therefore, it provides a reliable measure of the average size of a particle size distribution measured by DLS. The software assumes that the dispersion of the particles obey the Rayleigh theory (intensity of scattered light proportional to D_i^6) and the value of the average diameter of a distribution (corresponding to D_z) can be determined by Equation 2:

$$D_z = \frac{\sum(I_i)}{\sum(\frac{I_i}{D_i})} \quad \text{(Eq. 2)}$$

- D_z is the intensity weighted harmonic mean size of the hydrodynamic diameter distribution;
- I_i is the scattered light intensity of class i;
- D_i is the hydrodynamic diameter of class i.

.

The measured characteristic that defines the averaged molecular size of surfactant or particle size of a suspension is therefore the D_z. For the determination of this parameter, it is necessary to prepare a solution for an optimum concentration. The concentration chosen should always be as diluted as possible so that it is ensured that there is enough particles to

scatter enough light for the analysis, but trying to avoid the formation of aggregates and multiple scattering. The parameter *count-rate* that appears in the software of the ZSN gives this information and it was assured that this value was always greater than 50. With the increase in concentration, there is greater probability that inter-particles effects like multiple scattering will occur or the decrease in the free space between particles that leads to the emergence of friction forces between neighboring particles. The latter is an error factor because in DLS measurements it is assumed that the particles are moving only due to Brownian motion. Situations of multiple scattering can be detected through *quality report* produced by the software. As these situations vary for each material, it was necessary to try several concentrations until the optimal concentration was found. As this technique is used to determine size of molecules or aggregates of particles, the size of molecules of surfactants and particles of the dispersions can be determined.

Molecular weight measurement

Static light scattering (SLS) is a technique to measure absolute molecular weight using the relationship between the intensity of light scattered by a molecule and its molecular weight and size, as described by the Rayleigh theory. In simple terms, the Rayleigh theory says that larger molecules scatter more light than smaller molecules for a given light source, and that the intensity of the scattered light is proportional to the molecule's molecular weight [44]. Instead of measuring the time dependent fluctuations in the scattering intensity like in DLS, SLS uses the time-averaged intensity of scattered light.

From this information, the 2nd Virial coefficient and Molecular Weight could be determined. The 2nd Virial Coefficient is a property describing the strength of the interaction between the particles and the solvent or appropriate dispersant medium allowing us to measure the solubility of molecules. The molecular weight is determined by measuring the sample at different concentrations and applying the Rayleigh equation (Equation 3):

$$\frac{KC}{R_\theta} = \left(\frac{1}{MW} + 2A_2C\right)P_\theta \qquad \text{(Eq. 3)}$$

- K is the optical constant as defined in Equation 4;
- C is the concentration;
- R_θ is the Rayleigh ratio – the ratio of scattered light to incident light on the sample;
- MW is the sample molecular weight;

- A_2 is the 2nd Virial coefficient;
- P_θ is the angular dependence of the sample scattering intensity.

$$K = \frac{2\pi^2}{\lambda_o^4 N_A}\left(n_o \frac{dn}{dc}\right)^2 \quad \text{(Eq. 4)}$$

- N_A is the Avogadro's constant;
- λ_o is the laser wavelength;
- n_o is the solvent refractive index;
- dn/dc is the differential refractive index increment. It is the slope of the straight line obtained by plotting refractive indices versus sample concentration.

The standard approach for molecular weight measurements is to first measure the scattering intensity of the analyte used relative to that of a well described (standard) pure liquid with a known Rayleigh ratio. The standard used in this work was Toluene because it is suitable for precise measurements and R_θ is known over a range of wavelengths and temperatures. The expression used to calculate the sample Rayleigh ratio from a toluene standard is (Equation 5):

$$R_\theta = \frac{I_A\, n_o^2}{I_T\, n_T^2} R_T \quad \text{(Eq. 5)}$$

- I_A is the residual scattering intensity of the analyte;
- I_T is the toluene scattering intensity;
- n_T is the toluene refractive index;
- R_T is the Rayleigh ratio of toluene.

The angular dependence of the sample scattering intensity (P_θ) is a shape correction parameter that depends on the different positions of the same particle (cylinder, coil or sphere). This phenomenon occurs when particles are large enough to accommodate multiple scattering. However, when particles in solution are much smaller than the wavelength of incident light, multiple scattering will be avoided. Under these conditions P_θ is reduced to 1 and Equation 3 is an equation of a straight line in which the ordinate at the origin is 1/MW.

The final result of a MW test using SLS is a Debye plot. A typical plot is represented in Figure 10. This plot has two lines, Debye line (blue) and Intensity line (green). Both must

have a growing direction and the higher the correlation coefficient, the better the quality of the test. From the Debye line, the MW can be obtained at the intersection with the axis of null concentration. On the other hand, the intensity line allows to check if multiple scattering effects are present, which occur if the intensity of the scattered light decreases between two consecutive points when concentration increases. If this situation occurs, a new solution must be prepared with intermediate concentration, to eliminate the effect of multiple scattering.

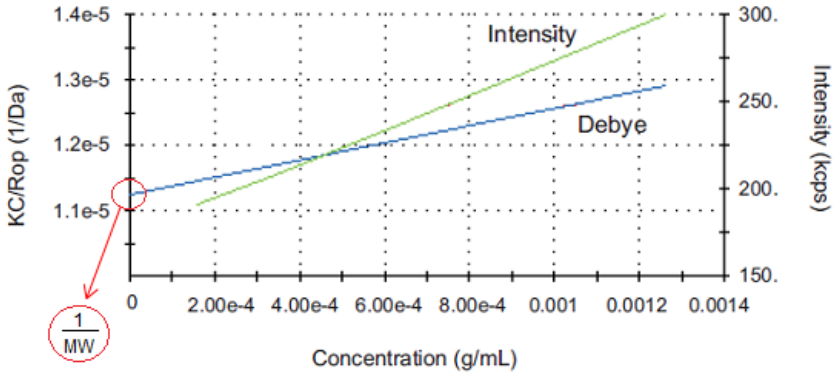

Figure 10 - Debye plot.

It can be seen that most of the parameters used in these calculations are constant, with the exception of the differential refractive index increment and dynamic viscosity, which must be introduced in the ZSN software. Information about the hydrodynamic diameter of the molecules can be introduced as well and then P_θ can have different values according to the position of particle expected.

Refractive index measurement

The refractive index (RI) is a dimensionless number defined as the ratio of the speed of light in vacuum and the speed of light in the targeted medium. RI was determined using a Refractometer (Atago RX-5000 CX) (Figure 11). For the determination of RI, the first step was the calibration with the solvent used (distilled water). Temperature was fixed at 25ºC. After this, two drops of the sample were placed on measuring cell for each tested concentration. Between each reading, the measuring cell should be cleaned with optical paper to avoid scratching. With all the RI's for the targeted concentrations determined, a regression of these values was made (refractive index versus surfactant concentrations) and the slope of straight line corresponds to the value of the dn/dc. Regression coefficient was always very high (above 0.97) as demonstrated in the Appendix A.

Figure 11 - Refractometer RX-5000D by Atago.

Dynamic viscosity measurement

The dynamic viscosity is the physical property that is associated with the intermolecular friction of a fluid and is reflected in its greater or lesser difficulty to flow at a given temperature. Determination of viscosity of surfactants has been made in a controlled stress reomether (Haake RS1) (Figure 12) where a cylindrical sensor with conical base (Z 34) was used. A recirculating bath was used to keep the temperature constant at 25ºC.

50 mL of the solution with the desired concentration were used for determination of viscosity. It was ensured that the cylindrical sensor was always fully immersed in the solution. The results obtained reflect values of dynamic viscosity as a function of shear rates. Considering the experimental variation, the dynamic viscosity remained constant except at very low shear rate. The final value of viscosity considered is the average of the values in the constant region.

Figure 12 - Controlled stress reomether of Haake, model RS1.

.

3.3.2 Characterization of surfactants

Hydrodynamic diameter of the molecules

In order to determine the molecular diameter for each surfactant, a 50 mL solution was prepared with 0.5% of each surfactant, i.e. 0.5 g/100 mL, from where samples were collected to be analyzed in the ZSN equipment. In this work all concentrations are specified by weight, so from now on when concentration is referred, it will be always by weight. The procedure of preparation of solutions was the following:

1) In a beaker, to the required amount of surfactant, water was added in a quantity not exceeding 50 mL (normally 40 mL) and then shacked for two hours, with the help of a magnetic stirrer (Figure 13 A), in order to promote a better particle dissolution of surfactant in water, forming the desired solution.

2) Two hours later the content was moved to a 50 mL dilution flask and was completed with water. The solution is ready for use (Figure 13 B).

3) With the help of a pipette, the surfactant solution was put in a square glass cell and introduced in the ZSN equipment (Figure 13 C). Temperature was set to 25ºC in the chamber.

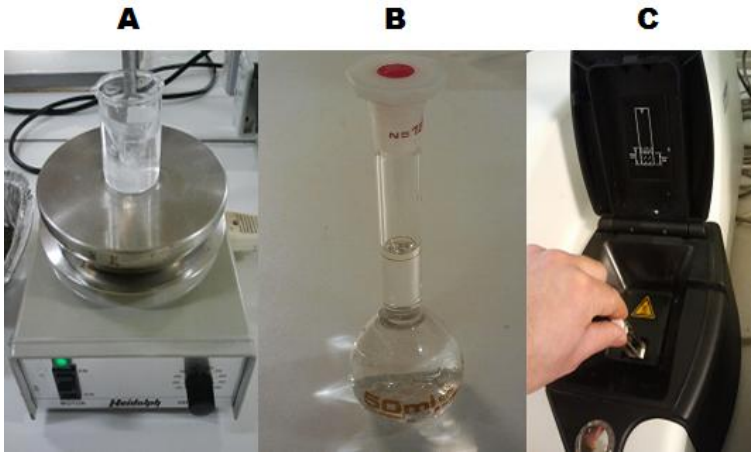

Figure 13 - Stages of preparation of a surfactant sample. Magnetic stirring in a beaker (A), dilution flask storage (B) and introduction of the ZSN equipment glass cell (C).

In order to ensure that the results are reproducible, all tests were performed on the equipment at least twice, and the end result adopted corresponds to the arithmetic average of all tests done in the same situation. Two tests were conducted for the surfactants Amber 4001, Glycerox and Disperse 31. In the case of surfactant Disperse 32, three tests were conduced because the intensity peaks were substantially smaller and larger variation was observed. All these distributions of intensity can be found in Appendix B.

For the same concentration used in determining the size of the molecules, viscosity and refractive index were also measured, as described in section 3.3.1. These values had to be introduced in the software to obtain the size distribuition. Table 3 summarizes the determined values for all four tested surfactants.

Table 3 - Refractive Index and Dynamic Viscosity.

Surfactant (-)	**Concentration (%)**	**Refractive Index (-)**	**Dynamic Viscosity (mPa.s)**
Glycerox	0.5	1.33413	1.81
Amber 4001	0.5	1.33375	1.83
Disperse 31	0.5	1.33401	2.42
Disperse 32	0.5	1.33357	1.91

In the cases of the surfactants Glycerox and Amber4001, size distributions meet the criteria of the quality report, the same does not happen for the surfactants Disperse 31 and Disperse 32 due to the multiple peaks obtained. In Figure 14 (A) is represented one of the distributions of surfactant sizes of Disperse 31, where it is verified the existence of three peaks of intensity, information on quality of analysis (quality report) and D_z (or Z-Average) calculated by the software. It is believed that the highest peak (of the order of 100 nm), corresponds to the existence of aggregates impossible to dissolve in the solution, so it was decided to remove it using the software of the ZSN and recalculated the value of D_z (Figure 14 B).

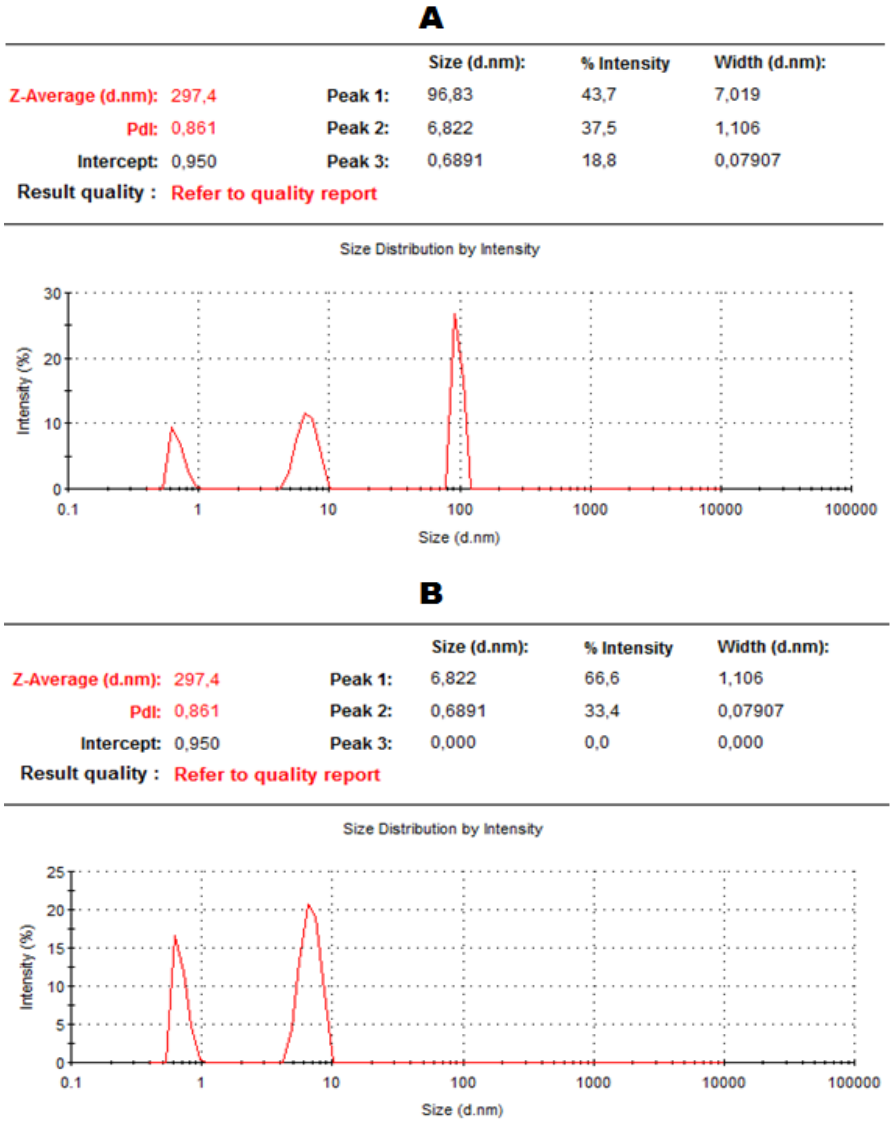

Figure 14 - Representation of the intensity of scattered light as a function of the diameter of the molecules and the information provided directly by the software ZSN (A) and edited by the user (B).

This procedure was repeated for all size distributions of surfactants Disperse 31 and Disperse 32 because there was always a clear peak showing aggregation of particles. Table 4 presents the averaged diameters of the surfactants molecules for all four surfactants tested.

Molecular weight

The procedure adopted for the determination of the molecular weight for each surfactant began with the preparation of four solutions of different concentrations. After this, the RI was determined for all concentrations as described in section 3.3.1 With the values of concentration and RI, it was possible to construct a plot of refractive index versus concentration to obtain the slope, dn/dc that was introduced in the software of the ZSN to

calculate the molecular weight. In Appendix A, it is possible to see the construction of regression lines and the values of the calculated slopes for each surfactant.

As also seen in section 3.3.1, the software starts by asking for the introduction of a sample with solvent, then a sample with the default reference toluene and only then asks for the various samples, with different concentrations values. These values must be manually inserted in the software. In the end, the results are returned in the form of a Debye plot which supplies a value of MW calculated by the ZSN software based on equation 3.

To ensure that no multiple scattering was present it was necessary to make several tries to determine the best concentrations for each surfactant. Reproducibility of the same results was somehow complicated, perhaps due to the high sensitivity of measurement. One of the major concerns was ensure that the cells were allways very clean and that no small air bubbles in the sample were present. To minimize the problem associated with the cleaning of the cells between the analyses of MW for the same surfactant, six different glass cells was used (one for the solvent, one for the standard and four for the various concentrations) and slight improvements were obtained at the level of reproducibility, although it was necessary to do a lot of tests to find reproducible results. All Debye plots built by the software can be found in Appendix C.

In Table 4, the values of the characterization made for surfactants in this study are summarized. Averaged values are indicated with ^{av}.

Table 4 - Summary of surfactants characterization.

Surfatant (-)	**D_z** (nm)	**D_z^{av}** (nm)	**MW** (kDa)	**MW^{av}** (kDa)
Glycerox	41,870	41,93	4950,00	4265,00
	41,980		3580,00	
Amber4001	5,735	5,65	58,00	54,25
	5,574		50,50	
Disperse31	1,694	2,41	11,20	8,78
	3,134		6,36	
Disperse32	3,330	3,28	26,60	24,75
	3,662		-	
	2,858		22,90	

3.3.3 Characterization of MWCNT dispersions

Once properly characterized, the assessment of the capacities of the surfactants studied to disperse MWCNT was proceeded. The method tested in this work for the dispersion of MWCNT consists in the addition of the MWCNT to a suspension of surfactant and subsequent application of ultrasonic energy. The only parameter that is intended to stud is the concentration of surfactant. The amount of MWCNT used was 0.01 g and kept constant in the MWCNT dispersions tests. The ultrasonication time will not be subjected to study. For a similar situation, Casaleiro [45] determined that the optimum value of ultrasounds time is 5 minutes, so this value has been adopted in the tests of the present work.

In the first stage, three solutions for each surfactant were prepared with different concentrations. It was seen in section 2.3.1, that with the increase in concentration of surfactant, the dispersion quality should improve, until a certain value of concentration, the optimum, from which the dispersion begins to produce poorer quality. The second stage involves the application of ultrasounds to make the most effective dispersion. The last stage corresponds to the assessment of the average size of each MWCNT dispersion, knowing that the smaller the particle size, the better the quality of dispersion (lower presence of aggregates).

The procedure followed for the evaluation of the dispersions quality was as follows:

1) Three solutions were prepared with 0.5, 1, and 3% of surfactant as described in section 3.3.2 for 150 mL of solution.

2) 0.01 g of MWCNT was added, to a 150 mL beaker with the solutions previously prepared.

3) The suspension in the beaker (aqueous solution of surfactant + MWCNT) was subjected to ultrasounds during 5 minutes, using a probe-sonicator (Sonics Vibracell 501), with a frequency of 20 kHz and power 500W, kindly provided by *Instituto Pedro Nunes* for use in this work. Casaleiro [45] verified that the simple application of ultrasounds increases the temperature of the suspension until 47ºC, promoting undesirable effects in the dispersion of MWCNT. In order to control this temperature rise, an external circuit was set up with coolant water in and out with the permanent addition of crushed ice to this guarantee, in this way, that the temperature of the suspension did not exceed 22ºC. Figure 15 presents all the apparatus used during this process, from the ultrasound probe to the cooling circuit with manual addition of crushed ice.

4) With the help of a pipette, the suspension put into the ZSN in glass cell which was introduced in the ZSN equipment, and the particle size test was carried out. This step was repeated for all concentrations of surfactant. Two measurements of each suspension were made.

Figure 15 - Apparatus used during the application of ultrasounds to the suspension.

3.3.4 UCS performance test

Performance tests were designed to demonstrate the applicability of MWCNT dispersion process and to characterize the mechanical performance of the soil stabilized with a binder enriched with MWCNT. In addition, the influence of the amount of MWCNT in the mechanical performance of the soil was also tested.

The experimental procedure involved two main phases: the preparation of molds with the samples and the test itself.

Sample preparation (phase 1)

1) Preparation of molds: molds are PVC pipes with inner diameter of 37 mm and height of 325 mm. In the inner walls of the base of the mold, vaseline was smeared in order to promote the sample slide. Duct tape was also glued to that region so that the sample does not come out of the mold. The duct tape had small holes to facilitate drainage. At the bottom it was introduced a geotextile circular filter.

2) Manual mixing of soil: the soil stored was removed from the thermo-hygrometric chamber and was homogenized manually (use of gloves indispensable) in such a way that the samples are representative of the entire soil.

3) Soil preparation: Approximately 900 g of soil was weighed, of which 840 g are left in the mixing bowl and the remaining mass is distributed by two capsules to assess the initial water content.

4) Binder preparative: In a plastic cup 98.942 g of Portland cement was weighed, to achieve a concentration of 175 kg of cement by cubic meter of soil.

5) Mixing: The cement was blended in a beaker with 150 mL of suspension (aqueous solution of surfactant + MWCNT), only with the aqueous solution of surfactant or only with water for the reference test. Then this mixture was put into the mixing bowl along with soil. With the use of a mechanical mixer (Hobart N50) at a rate of 136 rpm (Figure 16 A). The mixture was homogenized during three minutes. Halfway through the mixing process, mixing was stopped so that with the aid of spatulas the portions of material that had adhered to the walls of the mixing bowl were removed in order to ensure that the entire sample of soil was mixed with the syrup of binders. After complete mixing, a small portion was withdrawn of the mixture to assess the water content post-blending. The sample must be introduced in the mold straight away up to a maximum time of 30 minutes after mixing was stopped, otherwise there is a risk of the sample become a hard mass.

6) Compression: After molds are fixed to a support (Figure 16 B) began the insertion of fresh mixture into two molds was done in six layers simultaneously, each layer with 45 to 50 g. After the introduction in the mold of each layer, a slight compression was applied with a circular plate followed by application of vibration with the help of a drill to eliminate air bubbles within the mixture, followed by new slight compression. This process has always been applied to all 6 layers. In the end a new circular geotextile filter was applied to the top of the sample.

7) Curing: the molds with fresh samples were placed in a vertical position on a curing tank (Figure 16 C), filled with water at a temperature of 20 ± 2°C. During the curing period a vertical pressure of 24 kPa was applied at the top of each sample, in order to simulate actual field vertical effective stress at a depth of 5 m. The curing time for all samples was 7 days.

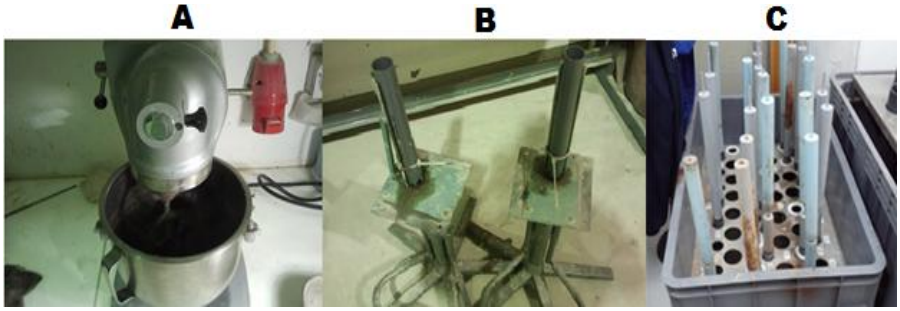

Figure 16 - Phases of sample preparation. Mixture (A) and molds where the sample was inserted (B) and curing tank (C).

UCS test (phase 2)

1) Extraction of specimen: After 7 days of sample preparation, the specimen was ready to be tested. For that the molds were taken from the curing tank and the specimens were demolded using an hydraulic extractor (Figure 17 A). The specimens were carefully cut so that they had a height of 76 mm and a height/diameter ratio of 2 (Figure 17 B).

2) Test preparation: The specimen was weighed for evaluation of the density. Then the specimen was carefully placed on the test press to ensure that the force was applied vertically and in the center of the specimen (Figure 17 C).

3) UCS test: It was defined a constant deformation rate of 1%/min in relation to the height of the specimen, which corresponds to 0.76 mm/min. During the test, the force applied to the specimen was automatically registered as a function of the displacement of the specimen, using a load cell and a displacement transducer, respectively. After reaching rupture, the specimen was removed from the test machine and two samples were picked up, to measure the final water content.

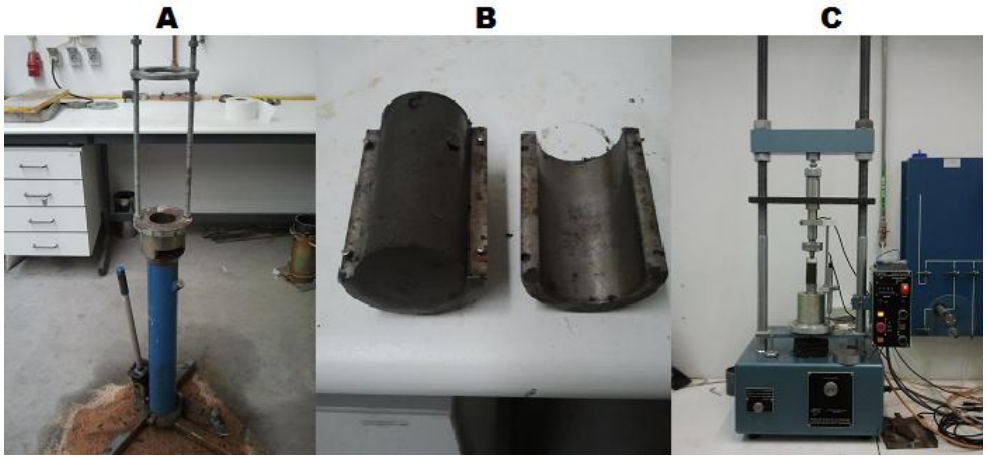

Figure 17 - UCS test stages. Hydraulic Extractor (A), specimen and mold (B) and testing press (C).

The force was converted to stress or unconfined compressive strength (q_u) which is obtained by the Equation 6.

$$q_u = \frac{F}{A} \quad \text{(Eq. 6)}$$

- q_u is the unconfined compressive strength;
- F is the force;
- A is the cross-sectional area of the sample.

The unconfined compressive strength is not more than a uniformly distributed force over an area A. The maximum force recorded during the test corresponds to maximum resistance of compressive sample ($q_{u\ max}$), and it is one of the parameters utilized to characterize the behavior of the soil chemically stabilized when subject to compression efforts. Stress-strain graphs (q_u-Ɛ) are constructed from the force exerted on the sample and vertical deformation based on sample geometry. In this way, the strain is calculated from the variation of the displacement considering valid the hypothesis of uniform distribution of deformation in the sample which is given by the Equation 7.

$$\varepsilon = \frac{\Delta\delta_v}{h} \times 100 \quad \text{(Eq. 7)}$$

- ε is the vertical strain;
- $\Delta\delta_v$ is the variation of the axial deformation;
- h is the height of sample.

The compression stress was calculated by the Equation 6, however the value of the cross-sectional area of the sample A should be a corrected value A_c in order to consider the radial deformation experienced by specimen [46]. A_c is given by Equation 8.

$$A_c = \frac{\pi \times D^2}{4 \times \left(1 - \frac{\varepsilon}{100}\right)} \quad \text{(Eq. 8)}$$

- A_c is the corrected cross-sectional area of the sample;
- D is the diameter of the sample.

3.4 Test plan

In order to study and characterize the influence of MWCNT dispersions (with surfactants Glycerox and Amber 4001) incorporated in the chemical stabilization of the soft soil in study, revealed by its mechanical behavior, a plan of tests that relied on unconfined compressive strength tests (UCS) was defined. The UCS tests aimed to study the behavior of the stabilized soil when subjected to compression efforts in a condition of non-confinement.

The information given by the characterizations of MWCNT dispersions led us to conclude that there was no need to test the surfactants Disperse 31 and Disperse 32, because they do not have the ability to disperse the MWCNT. As for the Glycerox, it was found that the optimal concentration should be between 1 and 3% of surfactant since better dispersion was obtained in this range. Thus, it was decided to test concentrations of 0.5, 1 and 2%. Regarding Amber 4001 it was found that the best dispersion was obtained with 3% and therefore it was decided to do tests with 0.5, 1 and 2% to compare with the Glycerox mixtures and with 3% because it corresponded to the best of the dispersions.

In Table 5 are presented the planned tests. A reference test where just water was added to cement was made. As surfactants can promote not only the dispersion of MWCNT but also the dispersion of the particles of soil and cement, tests only with surfactant for each concentration was performed. Finally tests with surfactant and MWCNT for each concentration of both were performed. The quantity of MWCNT added is defined by its content (ratio of the weight of MWCNT to the dry weight of cement), here expressed as concentration. Thus, MWCNT concentrations of 0.01% correspond to 0.01g/98.942g of Portland cement.

For each different test conditions, at least two specimens were tested. They were only validated if the range of variation of $q_{u\ max}$ was less than 15% of the average of the two values of $q_{u\ max}$.

Table 5 - Test plan for the surfactants Glycerox and Amber 4001.

Surfactant	Concentration (%)	MWCNT (%)
Glycerox	0.5	-
		0.001
		0.01
	1	-
		0.001
		0.01
	2	-
		0.001
		0.01
Amber 4001	0.5	-
		0.001
		0.01
	1	-
		0.001
		0.01
	2	-
		0.001
		0.01
	3	-
		0.001
		0.01

4 Results and discussion

4.1 Overview

This chapter presents and analyzes the results obtained for the characterization of dispersions of multi-wall carbon nanotubes (MWCNT) and their application in the chemical stabilization of soft soil of the low *Mondego* river.

All results presented below have been rigorously conducted to minimize experimental errors and promote the reproducibility of the results, as described in Chapter 3.

4.2 MWCNT dispersions

As referred in chapter 3, dispersions of MWCNT were prepared with four surfactants: Glicerox, Amber 4001, Disperse 31 and Disperse 32. Figure 18 shows the suspensions obtained using these four surfactants and for the three tested concentrations, immediately after application of ultrasonic energy. It can be clearly verified with the" naked eye", that the suspensions with surfactants Glycerox (Figure 18 A) and Amber 4001 (Figure 18 B) led to efficient dispersions of the MWCNT. On the other hand, the surfactants Disperse 31 and Disperse 32 (Figure 18 C) failed to disperse the MWCNT, and the presence of aggregates of MWCNT is obvious. It was concluded that the surfactants Disperse 31 and 32 were not indicated to promote the dispersion of the MWCNT, so these suspensions have not even been characterized.

The principal reason to explain these observations is the charge of the surfactants molecules. The zeta potential of the MWCNT (dispersed in a nonionic surfactant) was measured and the averaged value obtained was -25.5 mV, so clearly anionic. On the other hand, according to information from the supplier, Disperse 31 and Disperse 32 are both anionic having the same charge as the MWCNT, both anionic. So MWCNT particles and surfactant molecules will repulse each other due to electrostatic repulsions and surfactant adsorption and, consequently, dispersion will not be possible.

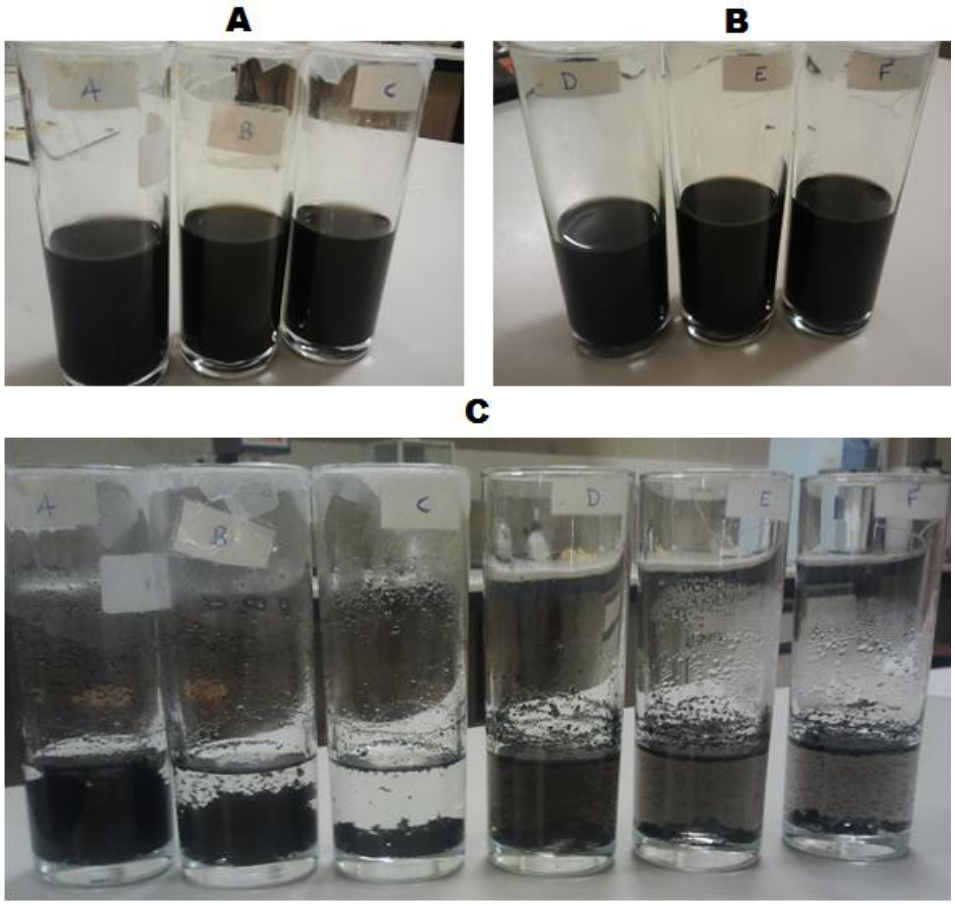

Figure 18 - MWCNT (concentration of 0.01%) dispersions in solutions enriched with Glycerox (A), Amber 4001 (B) and Disperse 31 and Disperse 32 (C) in cups A, B, C and D, E, F respectively, for concentrations of 0.5, 1 and 3% (from right to left).

The particle size distributions of MWCNT dispersed in aqueous solutions of Glycerox and Amber 4001, for concentrations of 0.5, 1 and 3% are presented in Appendix D and the summary of these results is presented in Table 6.

According to the supplier, Glycerox is a nonionic surfactant. Thus, Glycerox molecules will adsorb at negative surface of the MWCNT avoiding aggregation by steric stabilization.

In Figure 19 (A) one curve of particle size distributions of MWCNT for each concentration of Glycerox is presented. It was noted that for the concentration of 3% of surfactant, the range of the particles size is greater, so, there are smaller and larger particle in suspension. According to Table 6, D_z of the dispersions decreases between 0.5 and 1% but increases for 3%, justified by the presence of larger particles. So, the best concentration must be between 1 and 3%. This fact justifies the adoption of a concentration of Glycerox of 2% for the UCS performance tests, as discussed in the next section. The best MWCNT dispersion

is obtained for the concentration of 1% of surfactant, although the differences between the concentration of 1 and 3% of surfactant are small.

According to the supplier, Amber 4001 is a cationic surfactant, enabling an easy adsorption of the surfactant molecules at negative surface of the MWNCT, and avoiding aggregation by charge repulsion between surfactant molecules.

In Figure 19 (B) one curve of particle size distributions of MWCNT for each concentration of Amber 4001 is presented. It shows that concentrations of 1 and 3% of surfactant are similar and have behavior better than for 0.5% of surfactant Table 6 shows that D_z decreases with increasing concentration of the Amber 4001. However, once again, variation between concentrations of surfactant from 1 to 3% is small.

Table 6 - Summary of characterization of dispersions.

Surfactant (-)	**Concentration** (%)	**D_z** (nm)	**D_z^{av}** (nm)
Glycerox	0.5	195,500 / 198,900	197,20
	1	165,400 / 169,800	167,60
	3	184,200 / 166,200	175,20
Amber 4001	0.5	531,200 / 511,700	521,45
	1	322,300 / 323,400	322,85
	3	315,800 / 317,800	316,80

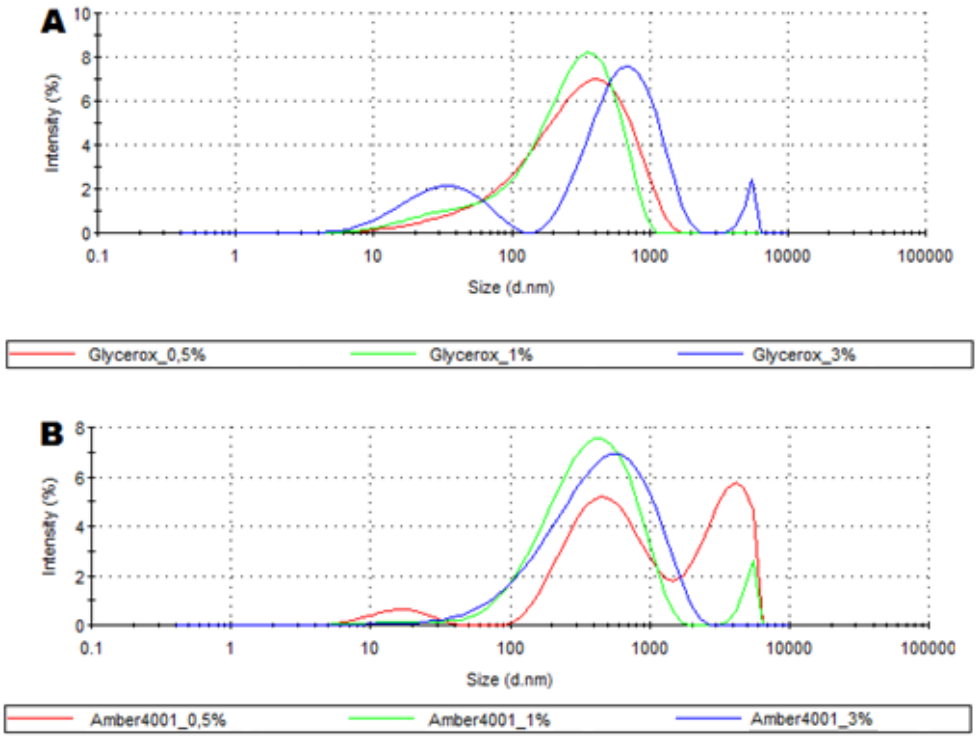

Figure 19 - Size distribution by intensity for the three concentrations tested of Glycerox (A) and Amber 4001 (B).

4.3 Application of MWCNT in soils

The results of the UCS tests, for dispersions of MWCNT applied in soft soil stabilization, planned in Chapter 3 are subsequently presented. Three main parameters will be studied: final water content (W_f) that is an indirect measure of the way that chemical reactions between cement and soil particles occurred, maximum stress ($q_{u\ max}$) that corresponds to the maximum point of each test giving information about the resistance of the sample and the secant undrained Young's modulus (E_{u50}), at 50% of the value of $q_{u\ max}$, which gives indication about the stiffness of the sample. The conclusions will be based on the averaged calculated values of pairs of tests (indicated with ^{av}). The variation of each test from the reference test was also calculated (indicated with ^{var}). Tables 7 and 8 contain the data for Glycerox and Amber 4001, respectively. Table 9 contains the data for the reference test (just water and cement were added to the soil), which allowed the evaluation of the E_{u50} and $q_{u\ max}$, presented in Tables 7 and 8. All the results are analyzed succinctly and a more detailed and integrated analysis is done in section 4.4.

The results have been grouped in order to analyze the influence of the amount of MWCNT and, after, in order to analyze the influence of the concentration of surfactant.

Table 7 - Results for the dispersions with Glycerox.

Surfactant (%)	MWCNT (%)	W_f (%)	W_f^{av} (%)	E_{u50} (MPa)	E_{u50}^{av} (MPa)	E_{u50}^{var} (%)	$q_{u\ max}$ (kPa)	$q_{u\ max}^{av}$ (kPa)	$q_{u\ max}^{var}$ (%)
0.5	0	80.35	79.6	15.43	16.4	4	151	163.0	14
0.5	0	78.85		17.35			175		
0.5	0.001	81.2	81.6	22.12	22.5	43	145	164.0	15
0.5	0.001	81.905		22.93			183		
0.5	0.01	80	80.7	17.03	16.1	2	185	184.5	29
0.5	0.01	81.3		15.26			184		
1	0	82.7	82.6	16.55	16.8	6	134	152.5	7
1	0	82.55		17.05			171		
1	0.001	82.15	83.6	26.71	27.6	75	184	174.0	22
1	0.001	85		28.49			164		
1	0.01	79	78.8	18.64	17.3	9	218	191.0	34
1	0.01	78.5		15.91			164		
2	0	80.4	80.6	20.57	19.9	26	179	173.5	21
2	0	80.75		19.32			168		
2	0.001	79.15	78.3	42.88	40.3	155	203	212.5	49
2	0.001	77.5		37.67			222		
2	0.01	77.45	78.7	20.61	20.7	31	238	229.0	60
2	0.01	79.85		20.74			220		

Table 8 - Results for the dispersions with Amber 4001.

Surfactant (%)	MWCNT (%)	W_f (%)	W_f^{av} (%)	E_{u50} (MPa)	E_{u50}^{av} (MPa)	E_{u50}^{var} (%)	$q_{u\,max}$ (kPa)	$q_{u\,max}^{av}$ (kPa)	$q_{u\,max}^{var}$ (%)
0.5	0	83.87	83.7	30.91	31.5	100	170	176.5	23
0.5	0	83.435		32.17			183		
0.5	0.001	84.6	83.7	36.69	36.0	128	205	225.0	57
0.5	0.001	82.8		35.39			245		
0.5	0.01	77.9	79.8	30.31	31.8	101	239	236.5	65
0.5	0.01	81.6		33.23			234		
1	0	83.7	82.3	30.88	31.9	102	199	206.0	44
1	0	80.9		32.85			213		
1	0.001	78.6	80.7	38.37	38.7	145	252	237.5	66
1	0.001	82.795		38.94			223		
1	0.01	80.72	80.4	33.7	34.2	116	240	252.5	77
1	0.01	80.005		34.61			265		
2	0	82.045	82.5	20.79	20.7	31	122	115.5	-19
2	0	82.97		20.68			109		
2	0.001	82.185	82.2	21.56	18.6	18	177	158.0	10
2	0.001	82.185		15.7			139		
2	0.01	82.96	82.6	17.85	19.2	22	122	123.5	-14
2	0.01	82.325		20.59			125		
3	0	82.6	82.3	8.78	9.2	-42	90	97.5	-32
3	0	81.9		9.65			105		
3	0.001	79.45	80.0	10.62	9.9	-37	123	131.0	-8
3	0.001	80.6		9.27			139		
3	0.01	81.55	82.5	9.14	7.8	-51	105	98.0	-31
3	0.01	83.35		6.43			91		

Table 9 - Results for the reference test.

W_f (%)	W_f^{av} (%)	E_{u50} (MPa)	E_{u50}^{av} (MPa)	$q_{u\,max}$ (kPa)	$q_{u\,max}^{av}$ (kPa)
79.65	81.1	16.17	15.8	157	143.0
82.6		15.41		129	

4.3.1 Influence of the MWCNT concentration

Figures 20 and 21 contain the UCS curves for the different MWCNT concentrations used, for the two surfactants studied, Glycerox and Amber 4001, respectively. For each test the two replicas are presented. Additionally, each graph also shows the reference curves (just water and cement were added to the soil) and also the curve corresponding to the tests only with surfactant and without MWCNT. The tests without MWCNT were made to distinguish the effects associated to the surfactant from the MWCNT.

In Figure 20 (A) the influence of the variation of MWCNT concentration in a solution of Glycerox at 0.5% is represented. At this low concentration of Glycerox, the $q_{u\,max}$ increases when compared with the reference test for samples with and without MWCNT. When the amount of MWCNT is increased from 0.001 to 0.01%, there is a slight increase of $q_{u\,max}^{var}$ to about 29%. At the low concentration of 0.5% of Glycerox, the increase in MWCNT content will not result in a substantial increase of $q_{u\,max}$ because it seems there are not enough molecules of surfactant to disperse all the MWCNT.

In Figure 20 (B and C) it is represented the influence of the MWCNT concentration when a solution of Glycerox at 1 and 2%, respectively, are used. As the MWCNT concentration increase, it was verified a proportional increment in $q_{u\,max}^{var}$ with the increase of the concentration of surfactant, from 22 to 34%, respectively, for the 1% of Glycerox and of 49 and 60% for the 2% solution of Glycerox. This means that for concentrations of Glycerox equal to 1 or 2%, there are enough molecules of surfactant to disperse the MWCNT, so the increase in MWCNT concentrations results in an increase of $q_{u\,max}$ thus in an increase of $q_{u\,max}^{var}$.

It was verified that no matter the concentration of Glycerox, the increase of MWCNT from 0.001 to 0.01%, makes the E_{u50} decrease. There is always an improvement of E_{u50} in relation with the reference test, even when only the surfactant is added but that improvement is the best for a concentration of MWCNT of 0.001%. The decrease of E_{u50}, with the increment of MWCNT seems to be justified by the increase of the number of nanoparticles which are accumulated in the cementitious bonds (probably in series arrangement). As the CNT exhibit large strains at failure, it means that when these MWCNT are arranged in series, they will promote the strain increase (when submitted to a stress increment), thus, the E_{u50} will decrease.

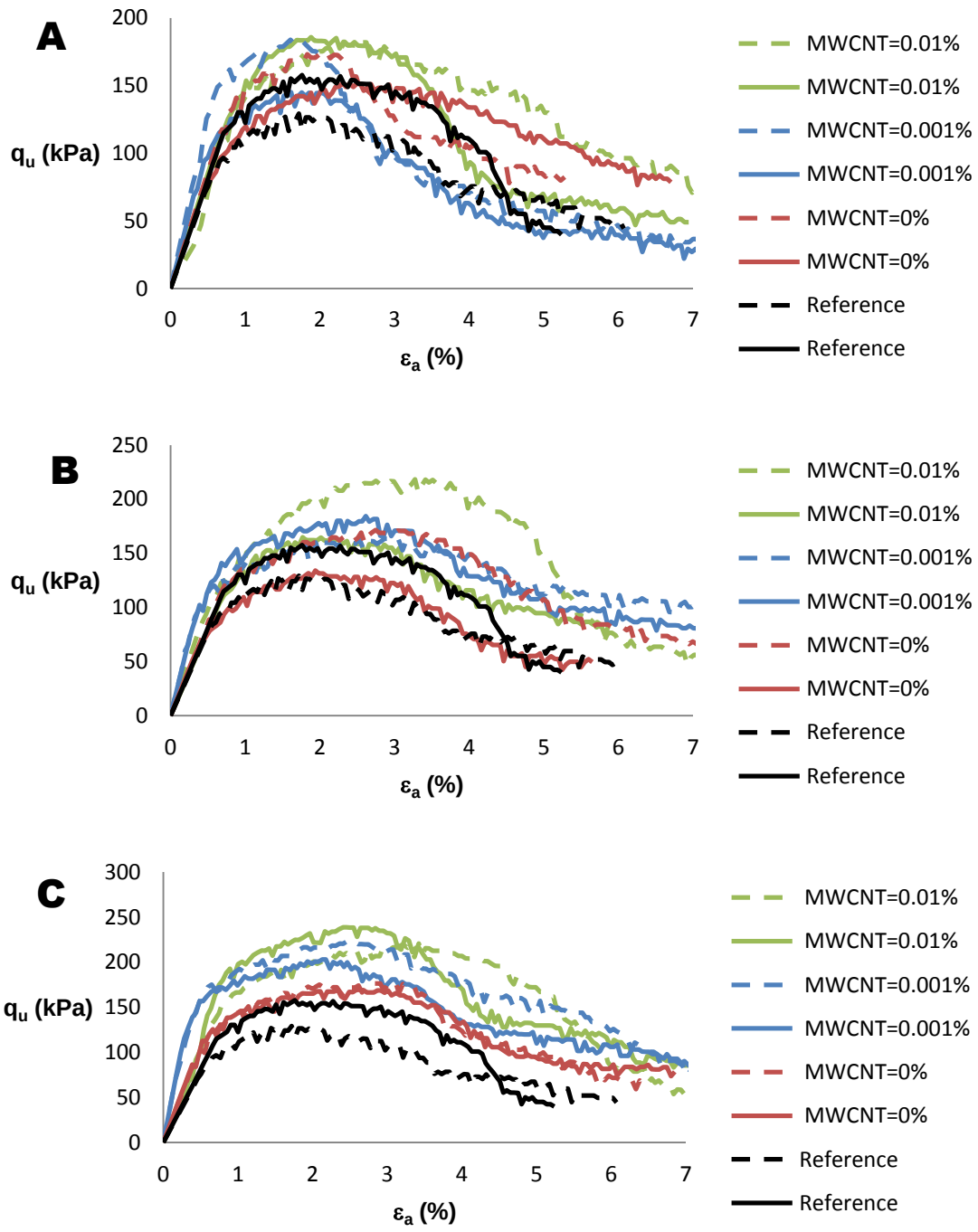

Figure 20 - Stress-strain graphs. Influence of the variation of the concentration of MWCNT in aqueous solutions of Glycerox with 0.5% (A), 1% (B) and 2% (C).

The influence of MWCNT concentration for all the selected concentrations of Amber 4001 is now analyzed. For concentrations of 0.5% (Figure 21 A) and 1% (Figure 21 B) of Amber 4001, the addition of MWCNT increases the $q_{u\ max}$ of the samples. In particular, at 1% of surfactant concentration, the addition of 0.01% of MWCNT results in an increase of $q_{u\ max}^{var}$ of 77%. At concentration of 2% (Figure 21 C), the introduction of 0.001% of MWCNT increases slightly $q_{u\ max}^{var}$ (10%), but at the concentrations of 3% (Figure 21 D), $q_{u\ max}^{var}$ is

always negative (decreases 8%) for a MWCNT concentration of 0.001%. The increase of MWCNT concentration to 0.01% makes further decrease of $q_{u\ max}$ in relation to the reference material, to start at concentration of 2% of surfactant.

Regarding E_{u50}, a similar situation to Glycerox has occurred for the concentrations of surfactant of 0.5 and 1%: the addition of MWCNT increases E_{u50} in both tests but the increase is higher with the addition of 0.001% of MWCNT than 0.01% of MWCNT. So, the increase in MWCNT does not favor the increase in E_{u50}. This increase is much higher than with Glycerox. For concentrations of 2% of surfactant there is a small increase of E_{u50} compared with the reference test, even if E_{u50} is higher, when only surfactant is added. For a surfactant concentration of 3% there is a decrease in E_{u50} for all situation, more pronounced for the higher MWCNT concentration.

For Amber 4001, it was concluded that, generally, the increase in MWCNT concentrations has a positive effect in $q_{u\ max}$ until the best concentration of surfactant which was identified as 1%. Concentrations higher than the best have a negative effect on the $q_{u\ max}$. However, the increase in MWCNT concentration above 0.001% has a negative effect in Eu_{50} for surfactant concentrations up to the best.

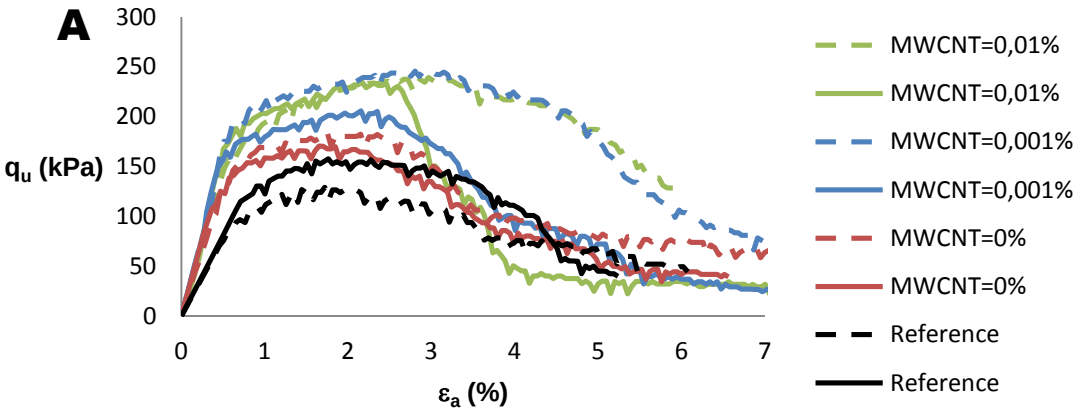

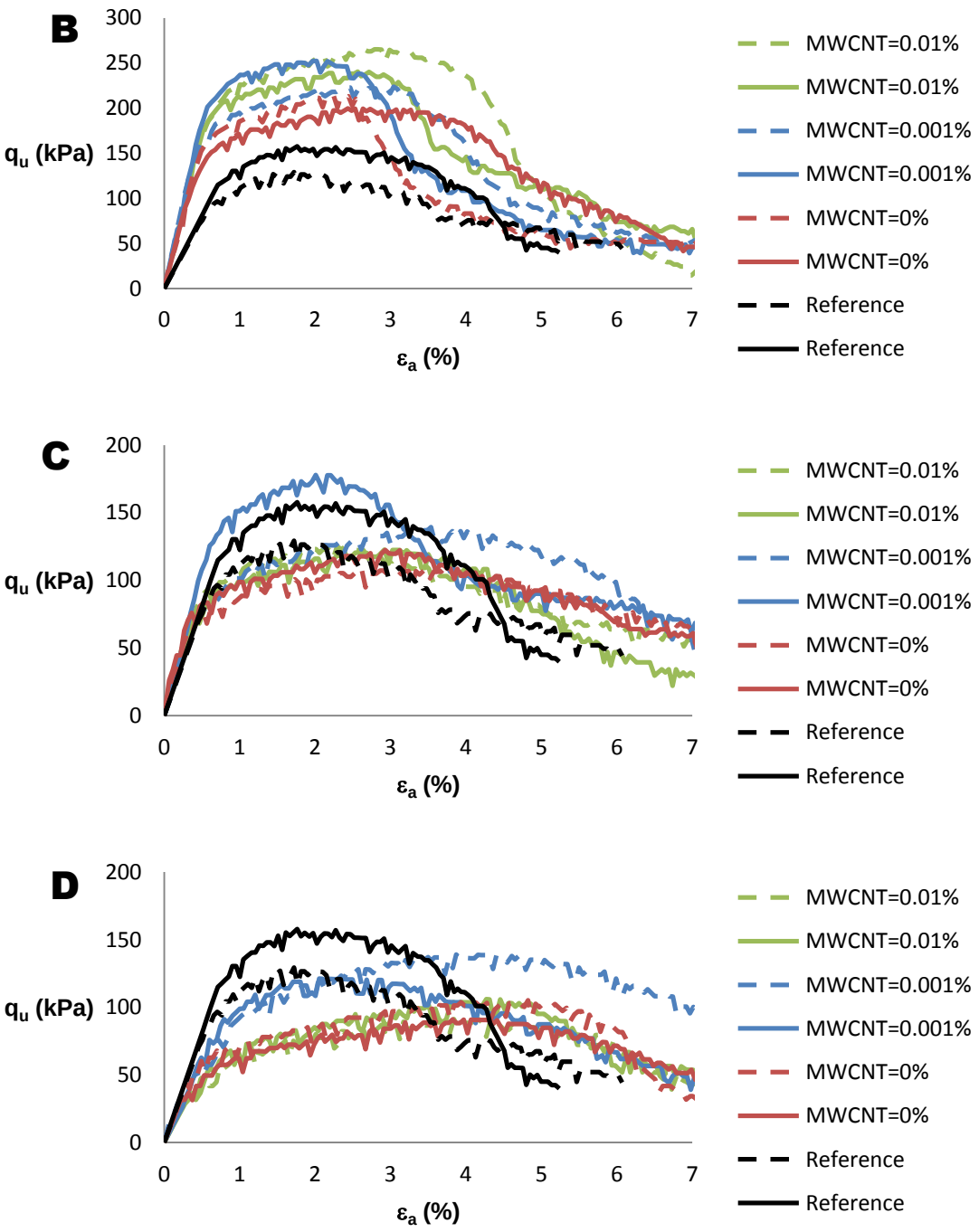

Figure 21 - Stress-strain graphs. Variation of the concentration of MWCNT in aqueous solutions of Amber 4001 with 0.5% (A), 1% (B), 2% (C) and 3% (D).

4.3.2 Influence of the surfactant concentration

Figures 22 and 23 represent the result of the UCS reference test and the results of the tests for the different concentrations of Glycerox and Amber 4001 respectively, for fixed concentration of MWCNT, as planned in chapter 3. Again, for each condition, the two replica tests are represented.

Figure 22 (A) represents the influence of Glycerox concentration in samples without MWCNT, i.e. samples where only surfactant and water were added to the mixture. It was verified that in all samples $q_{u\ max}$ increased in relation to the reference test. However, there is no defined trend on the $q_{u\ max}^{var}$ with Glycerox concentration. It can be said that the variations observed are within the experimental uncertainty. Additionally, for concentration of 1%, W_f is 2 to 3% higher than for the other concentrations, which might justify the lower $q_{u\ max}$ because it is well know that at high water soil stabilization, the $q_{u\ max}$ decreases as the water content increases [41]. The maximum value of $q_{u\ max}^{var}$ was 21% at 2% of Glycerox concentration.

It was also verified that the increase in Glycerox concentration increased slightly the E_{u50}^{var}, to a maximum of 26% at 2% of Glycerox. This slightly increase in E_{u50} might be due to the nonionic characteristic of Glycerox which has small interactions with cement particles.

In Figure 22 (B) the influence of variation of Glycerox concentration for samples with 0.001 % of MWCNT is represented. It was verified that the increase in Glycerox concentrations improves proportionally $q_{u\ max}$. The maximum value of $q_{u\ max}^{var}$ (49%) was obtained for 2% of Glycerox. The increase in Glycerox concentration leads to a significant increase on the E_{u50}^{var}, with a maximum of 155% at 2% of Glycerox.

In Figure 22 (C) the influence of the variation of Glycerox concentration for samples with 0.01 % of MWCNT is represented. This behavior is similar to the samples with 0.001% of MWCNT. However, now $q_{u\ max}^{var}$ are higher, with a maximum of 60%, again for 2% of Glycerox. Regarding the E_{u50}, there is also an improvement when the Glycerox concentrations increase, E_{u50}^{var} reaches a maximum of 31% at 2% of Glycerox. However, these values are lower than the ones obtained for the samples with 0.001% of MWCNT, as discussed previously.

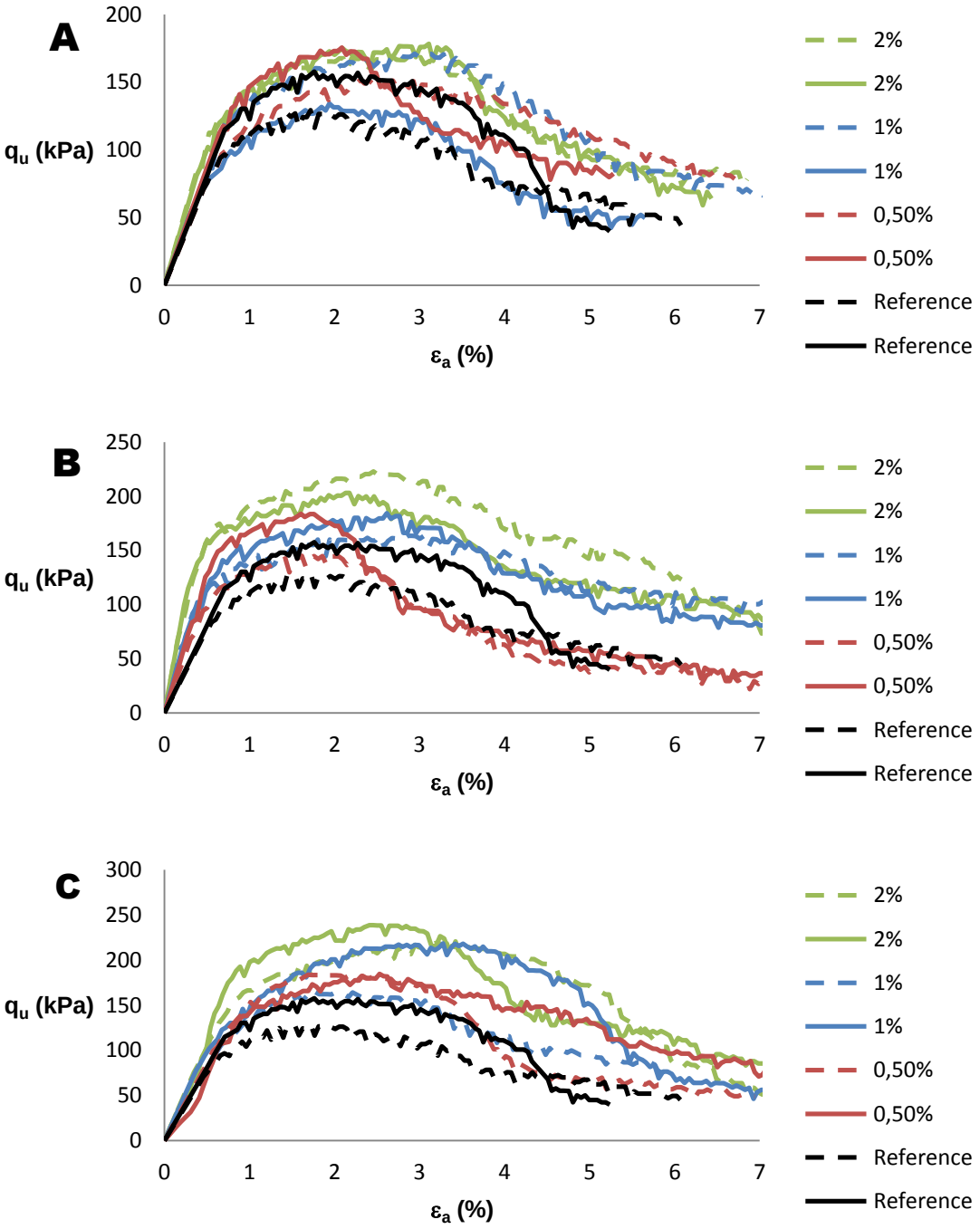

Figure 22 - Stress-strain graphs. Influence of the variation of the concentration of Glycerox in the absence of MWCNT (A), with 0.001% of MWCNT (B) and with 0.01% of MWCNT (C).

In Figure 23 (A) it is represented the influence of the variation of Amber 4001 concentration in samples without MWCNT, i.e. samples just with surfactant and water added to the mixture. In this case, it was verified that for concentrations of 0.5 and 1%, the $q_{u\ max}^{var}$ was 23 and 44%, respectively. On the other hand, for 2 and 3% of surfactant, a decrease of 19 and 32%, respectively, was achieved.

As for the E_{u50}, there was an increase in this parameter for concentrations of 0.5, 1 and 2%. This increase was similar and significant (around 100%) for 0.5 and 1% of surfactant and lower for a higher concentration of 2% (just 30%). For 3% of surfactant, a decrease of 32% was verified.

Figure 23 (B) represents the influence of the variation of Amber 4001 concentration when 0.001% of MWCNT was added. Again, it was verified an increase in $q_{u\ max}$ and E_{u50} until 1% of surfactant in solution. The increase in E_{u50}^{var} is more significant (145% for 1% of Amber 4001) than in $q_{u\ max}^{var}$ (66% for 1% of Amber 4001). From 2% of surfactant, the improvement in $q_{u\ max}^{var}$ and E_{u50}^{var} becomes smaller until it becomes negative for 3% of surfactant.

Figure 23 (C) represents the variation of Amber 4001 concentration when 0.01% of MWCNT was added to the mixture. A similar behavior to the one obtained with 0.001% of MWCNT was verified. The main difference is that the decrease of $q_{u\ max}$ starts at 2% of surfactant concentration. For the two lower concentrations of Amber 4001 (0.5 and 1%) the $q_{u\ max}$ was slightly higher for the highest concentration of MWCNT (0.01%).

It can be concluded that in general, the increase from 0.5 to 2% in Glycerox concentrations has a positive effect in $q_{u\ max}$ and E_{u50}. However, with Amber 4001 this positive effect was verified only until the concentration of 1% of surfactant. For concentrations higher than 2%, there is a detrimental effect on both $q_{u\ max}$ and E_{u50}.

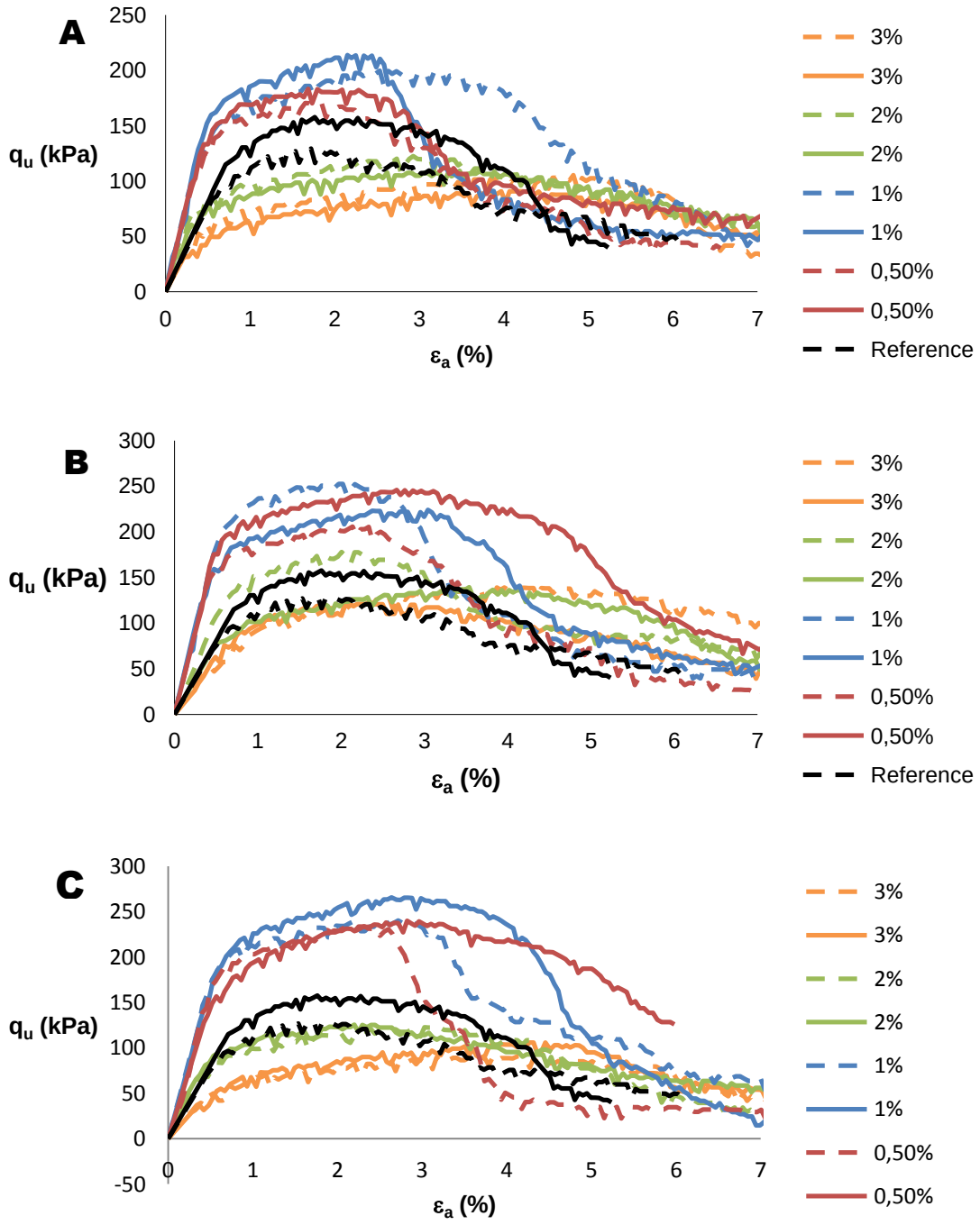

Figure 23 - Stress-strain graphs .Influence of the variation of the concentration of Amber 4001 in the absence of MWCNT (A), with 0.001% of MWCNT (B) and with 0.01% of MWCNT (C).

4.4 Discussion of results

After analyzing the results of the MWCNT dispersions (Table 6), it was found that the concentration of Glycerox which better could disperse the MWCNT was between 1 and 3%, while the best concentration of Amber 4001 for the same effect was 3%. Stabilized soil samples were prepared with Portland cement enriched with suspensions of MWCNT (0.001

and 0.01%) in solutions with 0.5, 1, and 2% in the case of Glycerox and in the case of Amber 4001, besides these concentrations a 3% concentration was also tested. In the case of the Glycerox (Table 7), it was found that there was a continuous improvement in the performance of UCS tests as the surfactant concentration increased up to 2%. In the case of Amber 4001 (Table 8), the suspension with best performance in the UCS tests was the one with 1% of surfactant and increasing this concentration further did decrease the performance in UCS tests.

Figure 24 represents the evolution of $q_{u\ max}$ with the concentration of Glycerox (A) and Amber 4001 (B) for each concentration of MWCNT (0.001 and 0.01%). Figure 25 represents the evolution of E_{u50} with the concentration of Glycerox (A) and Amber 4001 (B) for each concentration of MWCNT (0.001 and 0.01%).

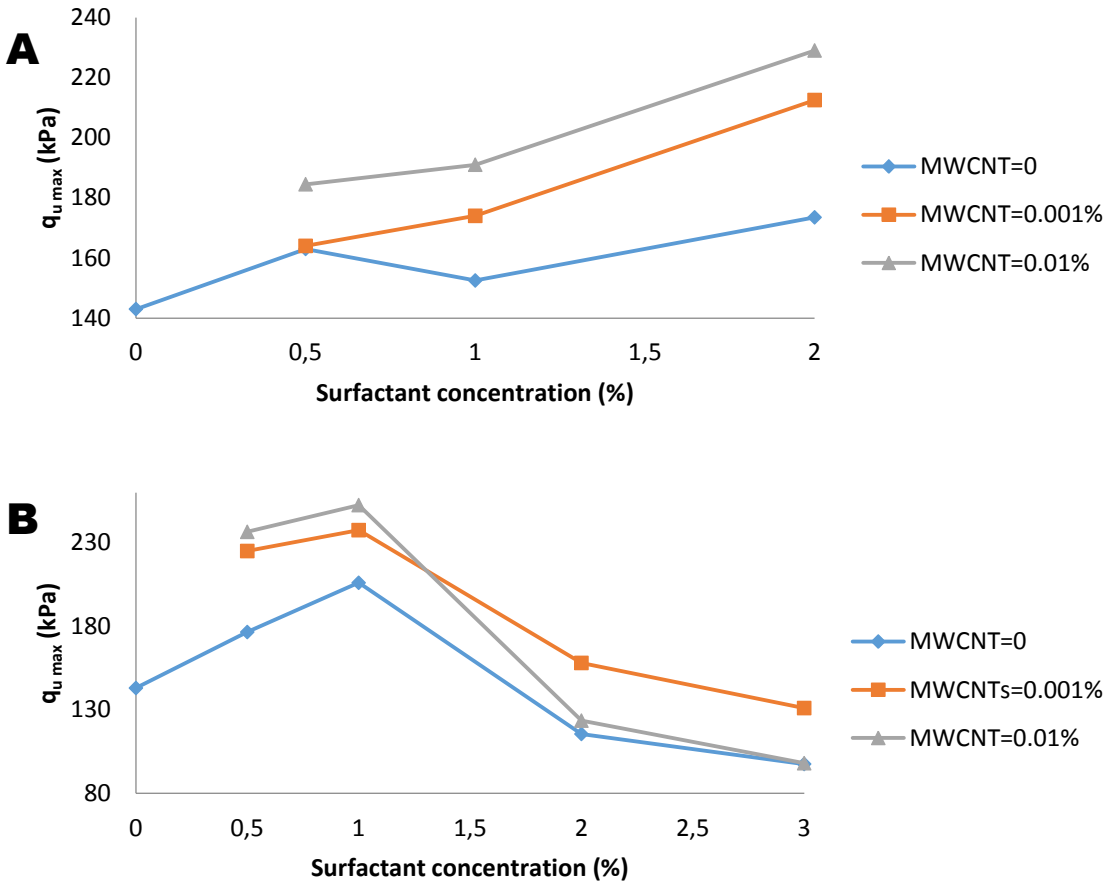

Figure 24 - Evolution of $q_{u\ max}$ with the concentration of Glycerox (A) and Amber 4001 (B) for each concentration of MWCNT.

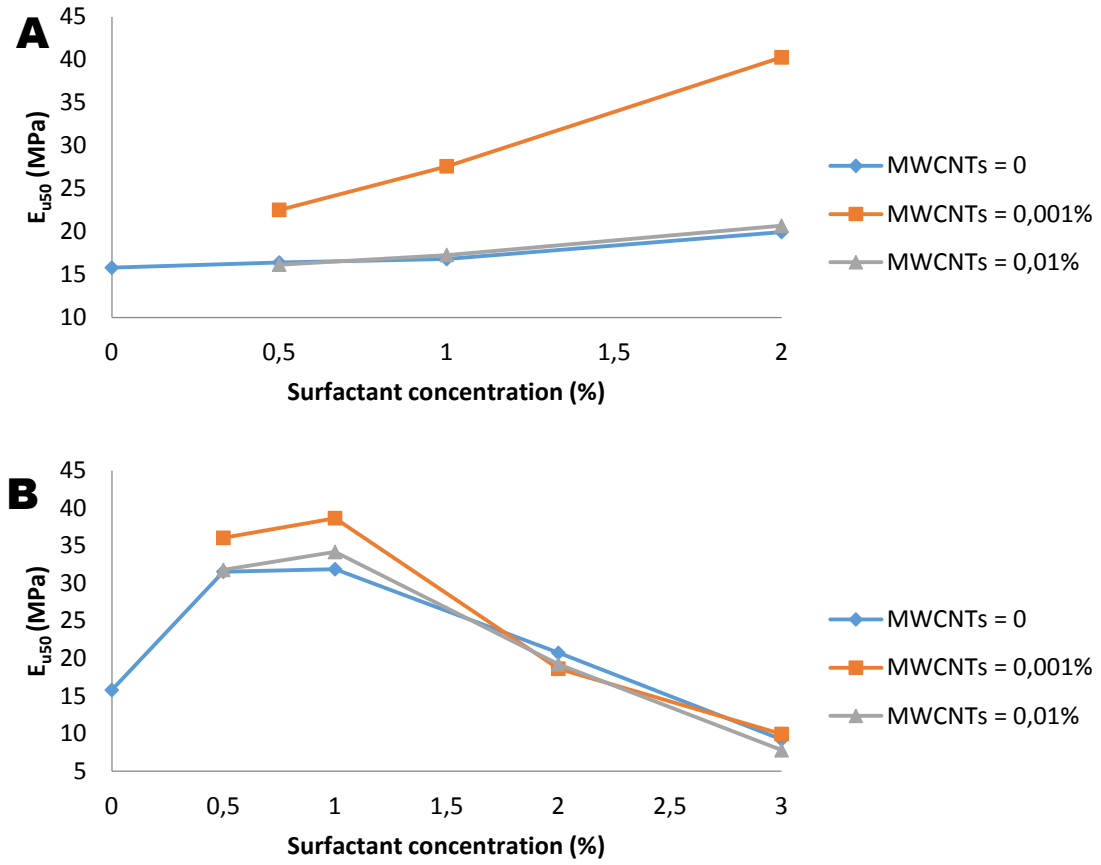

Figure 25 - Evolution of E_{u50} with the concentration of Glycerox (A) and Amber 4001 (B) for each concentration of MWCNT.

In the case of Glycerox, it was noted that the increase of $q_{u\ max}$ is related with the improvement of the dispersion of MWCNT. The maximum values of $q_{u\ max}$ occur for higher concentrations of MWCNT (0.01%) because good dispersions are achieved. Thus, it is possible to exploit this high quantity of MWCNT because they are effectively dispersed.

It was also noted that the addition of this surfactant has a negligible effect on the E_{u50}. However, the addition of small quantities of MWCNT (0.001%) leads to a huge improvement of E_{u50}. For these small quantities of MWCNT (0.001%), the matrix of cement and soil becomes denser, so the voids are filled by the MWCNT and E_{u50} increases. For the higher concentration of MWCNT (0.01%, correspondent to the presence of ten times more nanoparticles), the matrix becomes more dense and resistant (as proved by the $q_{u\ max}$ values), but as in the cement-soil bonding there are potentially more nanoparticles and as they have high strain at failure, their presence in higher quantities (in series arrangement) provides to the sample a ductile behavior, decreasing the stiffness and thus, E_{u50}. This justification is proved by the extended behavior (more ductile) of the graphs stress-strain when the concentration of MWCNT is increased.

In the case of surfactant Amber 4001, the fact that the best dispersion is found for concentrations of 3% while, in the UCS tests, the best performance is for concentrations of 1% seems to be contradictory. However, these situations may not be comparable due to the differences between the medium where the dispersions occurs. In the first case, the dispersions were evaluated in a medium where MWCNT were mixed only with the aqueous solution of surfactant. For the UCS tests, these dispersions were placed in a totally different environment where, besides the soil particles (more or less homogenized), there were also cement particles reacting chemically with water.

For concentrations of Amber 4001 above 1%, it seems that critical micelle concentration (CMC) may have been exceeded. As a result, there are too many molecules of surfactant, which instead of adsorbing on the surface of the MWCNT to promote their dispersion, may start to form micelles, which in a medium with large particles like soil particles and cement particles, can make the reactions between cement and water more difficult decreasing the mechanical behavior of the final samples. The same effect is present when only Amber 4001 is mixed with soil and cement. Moreover for concentrations of 2 and 3% of surfactant, samples become more viscous which also contributes to make hydration reactions more difficult. Still, for concentrations of Amber 4001 up to 1% the improvement in $q_{u\ max}$ is higher than for the case of Glycerox. This may be attributed to the cationic charge of Amber 4001 which favors adsorption to the cement particles, in opposition to the nonionic nature of Glycerox, if concentration is kept below the CMC. This justification is matches the occurrence of a maximum of 1% in Figure 24 (B) even when MWCNT are not added to the mixture.

Regarding the capacity of Amber 4001 to disperse MWCNT for concentrations above 1%, apparently above CMC, the fact is that formation of micelles is not necessarily detrimental for the dispersion capacity of a certain surfactant (Table 6). In fact, those micelles can even favor the dispersion of the MWCNT. However, once in a different environment (soil-cement), such concentrations of Amber 4001 (>1%) seem to render reactions between cement and water more difficult (Table 8).

It was also noted that the addition of this surfactant leads to an increase on the E_{u50} up to the concentration of 1% of surfactant. Once again this proves that Amber 4001 has good ability to disperse cement particles until concentration of surfactant of 1%. Above this concentration, a negligible increase for 2% of surfactant and a decrease for 3% of surfactant on the $E_{u50,}$ in relation of micelles, hinder the cementitious reactions. Regarding the influence of the concentration of MWCNT on E_{u50}, it is similar to the behavior observed for Glycerox

until 1% of Amber 4001. Above 1% of surfactant, the effect of the presence of surfactant overlaps the effect of MWCNT and E_{u50}values seems to be independent of the concentration of MWCNT.

Soft soils have high levels of porosity, caused by the usually large volume of voids between soil particles. The addition of cement to the soil allows the filling of those free spaces establishing bonds with soil particles, building a more resistant solid matrix, increasing the mechanical properties of soil. If cement is enriched with MWCNT, the increase of mechanical properties can be further enhanced due to the excellent mechanical properties of MWCNT, as long as a good dispersion is ensured. However, it was generally verified that the increase of MWCNT concentrations increased $q_{u\ max}$ and decreased E_{u50}. This can be explained due to the properties of MWCNT which have very high strength with large strains at failure, so the increase in MWCNT concentration will promote the strain increase, thus the E_{u50} will decrease.

While Glycerox has poor ability to disperse large particles like cement particles without the presence of MWCNT, Amber 4001 has good ability to disperse these particles. This can be explained because of the charge of surfactants and cement particles. As cement is negatively charged, a cationic surfactant as Amber 4001 can easily be adsorbed on the surface of cement particles, resulting in a better dispersion of these particles in suspension. The dispersion of cement particles will thus lead to a better filling of “free” spaces between soil particles building a solid matrix even more resistant.

Thus, the most advantageous surfactant is Amber 4001, which besides being the surfactant with overall better results in UCS tests, with a maximum of 77% in $q_{u\ max}^{var}$ and 145% in E_{u50}^{var}, is also the surfactant for which a smaller quantity (1%) is necessary to obtain the best results (best compromise of $q_{u\ max}$ and E_{u50}).

5 Conclusions and future work

5.1 Conclusions

In this work, cementitious composites reinforced with MWCNT were developed and applied to soft soil to improve its mechanical properties.

Effective reinforcement is possible only if good dispersions of MWCNT are guaranteed. Results showed that anionic surfactants (Disperse 31 and Disperse 32) are not effective to disperse MWCNT. On the other hand, a cationic (Amber 4001) and a nonionic (Glycerox) surfactant are effective to disperse MWCNT, which is explained by the fact that MWCNT are negatively charged. Also the fact that Glycerox and Amber 4001 are surfactants with higher hydrodynamic diameters and molecular weight can help explain these results.

Based on UCS tests, the influence of MWCNT concentration and surfactant concentration (Glycerox and Amber 4001) on compressive strength and undrained secant Young's modulus were evaluated.

Results showed generally that the increase in MWCNT concentrations has a positive effect in $q_{u\ max}$ until optimum concentration of surfactant. Concentrations of surfactant higher than the optimum have a negative effect on the value of $q_{u\ max}$. However, for the higher MWCNT concentration tested the values of E_{u50} were lower, even for surfactant concentrations up to the optimum, which is explained by the MWCNT properties (high strength with large strains at failures).

Results also showed that the increase from 0.5 to 2% in Glycerox concentrations has a positive effect in $q_{u\ max}$ and E_{u50}. However, for Amber 4001 this positive effect was verified only for concentrations up to 1%. For concentrations higher than 1%, the increase of surfactant concentration leads to a decrease in both $q_{u\ max}$ and E_{u50}, reaching values below the ones of the reference test. This behavior was justified by the presence of micelles for concentration above 1%, which can make the reactions between cement and water more difficult.

The maximum value for $q_{u\ max}$ (increase of 77% in relation to the reference test, with no surfactant and no MWCNT) was verified for 0.01% of MWCNT and 1% of Amber 4001 and the maximum value for E_{u50} (increase of 155% in relation to the reference test, with no surfactant and no MWCNT) was verified for 0.001% of MWCNT and 2% of Glycerox,

Thus, it can be concluded that the addition of MWCNT effectively dispersed in a suspension improves the mechanical properties of a soft soil stabilized with cement. However,

the charge and concentration of surfactant and the amount of MWCNT added have a crucial influence on the final properties of the composite.

5.2 Future works

The work developed responded to the initial goals. However, there is still much to explore around the theme of this work. Some proposals are given below:

- Others surfactants with different chain architecture, molecular weight and hydrodynamic diameter should be tested to check if better dispersions can be obtained and their effect on the mechanical properties of soil should be analyzed;
- A more extended and detailed study on the effect of the concentration of surfactant and MWCNT should be done, extending the range of concentrations evaluated;
- The same dispersions tested in this study should be applied in other composites of different soils to conclude if it is possible to generalize the conclusions that were obtained in the present work.

6 References

1. S. Iijima. "*Helical microtubules of graphitic carbon"*, Nature (London), 354; pp 56-58 (1991).
2. H. Golnabi. "*Carbon nanotube research developments in terms of published papers and patents, synthesis and production"*, Scientia Iranica, 19(6); pp 2012-2022 (2012).
3. S. Iijima. "*Carbon nanotubes: past, present, and future"*, Phys. B-Condens. Mat., 323(1-4); pp 1-5 (2002).
4. S. Iijima, T. Ichihashi. "*Single-shell carbon nanotubes of 1-nm diameter"*, Nature (London), 363; pp. 603-605 (1993).
5. D.S. Bethune, C.H. Kiang, M.S. Devries, G. Gorman, R. Savoy, J. Vazquez, R. Beyers. "*Cobalt-catalysed growth of carbon nanotubes with single-atomic-layer walls"*, Nature, 363; pp 605-607 (1993).
6. N. K. Mehra, V. Mishra, N.K. Jain, *A review of ligand tethered surface engineered carbon nanotubes.* Biomaterials, 35(4); pp 1267-1283 (2013).
7. R.H. Baughman, A.A. Zakhidov, W.A. De Heer. "*Carbon nanotubes – the route toward applications"*, Science, 297(5582); pp 787-792 (2002).
8. L. Vaisman, H.D. Wagner, G. Marom. "*The role of surfactants in dispersion of carbon nanotubes"*, Advances in colloid and interface science, 128-130; pp 37-46 (2006).
9. P. Newman, A. Minett, R. Ellis-Behnke, H. Zreiqat. "*Carbon nanotubes: Their potential and pitfalls for bone tissue regeneration and engineering"*, Nanomedicine: Nanotechnology, Biology, and Medicine, 9(8); pp 1139-1158 (2013).
10. E. Flahaut, R. Bacsa, A. Peigney, C. Laurent. "*Gram-Scale CCVD synthesis of double-walled carbon nanotubes"*, Chemical communications, 12; pp 1442-1443 (2003).
11. X.L. Xie, Y.W. Mai, X.P. Zhou. "*Dispersion and alignment of carbon nanotubes in polymer matrix: A review"*, Materials science & Engineering: R: Reports, 49(4); pp 89-112 (2005).
12. V. Choudhary, A. Gupta. *"Polymer/Carbon Nanotube Nanocomposites"*, Carbon Nanotubes - Polymer Nanocomposites, Siva Yellampalli, (2011).
13. F. Sanchez, K. Sobolev. *"Nanotechnology in concrete – A review"*, Construction and Building Materials, 24(11); pp 2060-2071 (2010).
14. V. Choudhary, S.K. Dhawan, P. Saini. "*Polymer based nanocomposites for electromagnetic interference (EMI) shielding"*, Polym. Advn. Technol, 21; p 1 (2010).

15. N. M. Mubarak, J. N. Sahu, E.C. Abdullah, N.S. Jayakumar. "*Removal of heavy metals from wastewater using carbon nanotubes"*, Separation & Purification Reviews, 43(4); pp 311-338 (2014).
16. E.C. Bradley, W. A. Westling. "*The space elevator"*, A Revolutionary Earth-to-Space Transportation System (2003).
17. A. Beigbeder, P. Degee, S. Conlan, R. Mutton, A. Clare, M. Pettitt, M. Callow, J. Callow, P. Dubois. "*Preparation and characterization of silicone-based coatings filled with carbon nanotubes and natural sepiolite and their application as marine fouling-release coatings"*, Biofouling, 24; pp 291-302 (2008).
18. J.M. Planeix, N. Coustel, B. Coq, V. Brotons, P.S. Kumbhar, R. Dutartre, P. Geneste, P. Bernier, P.M. Ajayan. "*Application of carbon nanotubes as supports in heterogeneous catalysis"*, J. Am. Chem. Soc., 116(17); pp 7935-7936 (1994).
19. G. Che, B.B Lakshmi, E.R. Fisher, C.R. Martin. "*Carbon nanotubule membranes for electrochemical energy storage and production"*, Nature, 393; pp 346-349 (1998).
20. J. Kong, N.R. Franklin, C. Zhou, M.G. Chapline, S. Peng, K. Cho, H. Dai. "*Nanotube molecular wires as chemical sensors", Science*, 287; pp 622-625 (2000).
21. P.G. Collins, K. Bradley, M. Ishigami, A. Zettl. "*Extreme oxygen sensitivity of electronic properties of carbon nanotubes"*, Science, 287(5459); pp 1801-1804 (2000).
22. M.S. Konsta-Gdoutos, Z.S Metaxa, S.P. Shah. "*Multi-scale mechanical and fracture charateristics and early-age strain capacity of high performance carbon nanotube/cement nanocomposites"*, Cement and Concrete Composites, 32(2); pp 110-115 (2010).
23. M.S. Konsta-Gdoutos, Z.S. Metaxa, S. P. Shah, P. Mondal. "*Nanoscale modification of cementitious materials"*. In: Z. Bittnar, P.J.M. Bartos, L. Nemecek, V Smilauer, J. Zeman, Editors: Nanotechnology in construction. Proceedings of the Third International Symposium on Nanotechnology in construction. Prague. Czech Republic; pp 125-130 (2009).
24. M.S. Konsta-Gdoutos, Z.S. Metaxa, S.P. Shah. "*Carbon nanotubes reinforced concrete, nanotechnology of concrete: The next big thing is small"*, SP-267, American Concrete Institute, Farmington Hills, MI; pp. 11-20 (2009).
25. M.S. Konsta-Gdoutos, Z.S. Metaxa, S.P. Shah. "*Nanoimaging of highly dispersed carbon nanotube reinforced cement based materials*", Proceedings of the Seventh International RILEM Symposium on Fiber Reinforced Concrete: Design and Applications, R. Gettu, ed., RILEM Publications S.A.R.L.; pp 125-131 (2008).

26. R. Abu Al-Rub, B. Tyson, A. Yazdanbakhsh, Z Grasley. "*Mechanical properties of nanocomposite cement incorporating surface-treated and untreated carbon nanotubes and carbon nanofibers"*, J. Nanomech. Micromech., 2(1); pp 1-6 (2012).
27. M.S. Konsta-Gdoutos, Z.S. Metaxa, S.P. Shah. "*Highly dispersed carbon nanotube-reinforced cement-based materials"*, Cement and Concrete Research, 40(7); pp 1052-1059 (2010).
28. V.C. Moore, E.H. Haroz, M.S. Strano, R.H. Hauge, R.E. Smalley, J. Schmidt, Y. Talmon. "*Individually suspended single-walled carbon nanotubes in various surfactants"*, Nano Letters, 3(10); pp 1379-1382 (2003).
29. M. D. Rossell, C. Kuebel, G. Ilari, F. Rechberger, F.J. Heiligtag, M. Niederberger, D. Koziej, R. Erni. "*Impact of sonication pretreatment on carbon nanotubes: A transmission electron microscopy study"*, Carbon, 61; pp 404-411 (2013).
30. Y. Lestari, G. Ramadhan, A.Y. Akbar, S. Bahri, E. Martides, E. Sugiarti, D.S. Khaerudini. "*Effect of different dispersants in compressive strength of carbon fiber cementitious composites"*, AIP Conf. Proc. 1555, 67 (2013).
31. M. Kitazume, M. Terashi. "*The deep mixing method – principle, design and construction"*. Coastal Development Institute of Technology, Japan. Balkema. (2002).
32. L. Chen, D. F. Lin. "*Stabilization treatment of soft subgrade soil by sewage sludge ash and cement"*, Journal of Hazardous Materials, 162(1); pp. 321-327 (2009).
33. A. Yague, S. Valls, E. Vazquez. "*Use of cement Portland mortar of stabilized dry sewage sludge in construction applications"*, Waste Manage. Environ; pp 527-536 (2002).
34. D.F. Lin, H.L. Luo, S.W. Zhang. "*Effects of nano-SiO2 on tiles manufactured with clay and incinerated sewage sludge ash"*, J. Mater. Civil Eng., ASCE 19(10); pp 801-808 (2007).
35. C.H. Hurley, T.H. Thornburn. "*Sodium Silicate Stabilization of Soils: A Review of the Literature"*. Highway Research Record, (381); pp 46-79 (1972).
36. A. M. Neville. "*Properties of Concrete"*, ELBS and Longman, Malaysia, 4th edition, (1996).
37. B. J. Elliott, M. Gilmore. "*Fiber Optic Cabling*", Newnes, 2nd edition; (2002).
38. . R. Varadaraj, J. Bock, S. Zushma, N. Brons, T. Colletti."*Effect of hydrocarbon chain branching on interfacial properties of monodisperse ethoxylated alcohol surfactants*", Journal of Colloid and Interface Science, 147(2); pp 387-395 (1991).

39. M. Achouri, S. Alehyen, A. Assioui, R. Chami, F. Bensajjay, L. Pérez, M. Infante. "*Synthesis and Physico-Chemical Studies of Ester-Quat Surfactants in the Series of (Dodecanoyloxy)propyl n-Alkyl Dimethyl Ammonium Bromide*", Journal of Surfactants and Detergents, 16(4); pp 473-485 (2013).

40. S. Srinivasan, S.A. Barbhuiya, D. Charan, S.P. Pandey. "*Characterising cement–superplasticiser interaction using zeta potential measurements*". Construction and Building Materials, 24(12); pp 2517-2521 (2010).

41. A.A.S. Correia, "*Aplicabilidade da Técnica de Deep Mixing aos Solos Moles do Baixo Mondego*". PhD Thesis, Department of Civil Engineering of FCTUC, Coimbra (2011).

42. Malvern, http://www.malvern.com/en/products/product-range/zetasizer-range/zetasizer-nano-range/zetasizer-nano-zs/default.aspx (Retrieved January 7th, 2014)

43. Malvern, http://www.malvern.com/en/products/technology/dynamic-light-scattering (Retrieved January 10th, 2014)

44. Malvern, http://www.malvern.com/en/products/technology/static-light-scattering (Retrieved January 11th, 2014)

45. P.D.F. Casaleiro, "*Estabilização química do Solo Mole do Baixo Mondego por recurso a nanomateriais*". Master's Thesis, Department of Civil Engineering of FCTUC, Coimbra (2014).

46. K.H. Head, "*Manual of soil laboratory testing*". Vols. 1, 2 e 3, Pentech Press, London, (1985).

Appendix

Appendix A

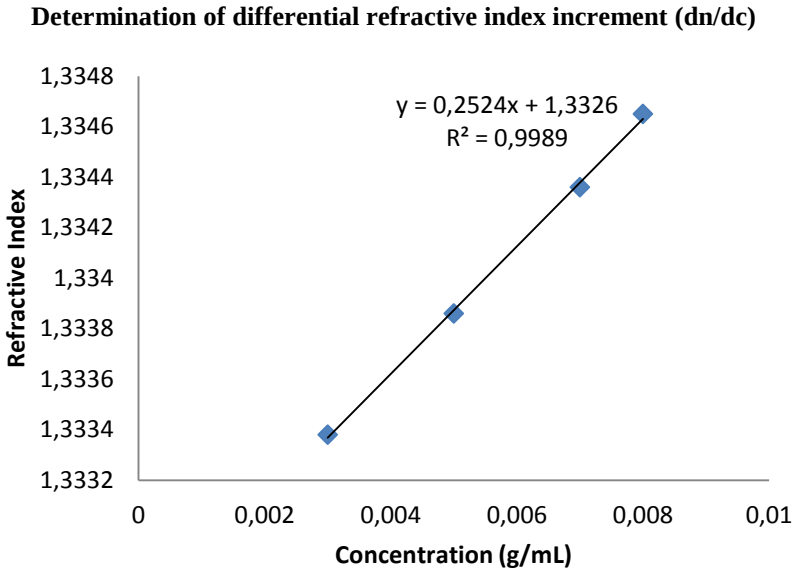

Figure A1- Determination of the dn/dc parameter to the surfactant Glycerox.

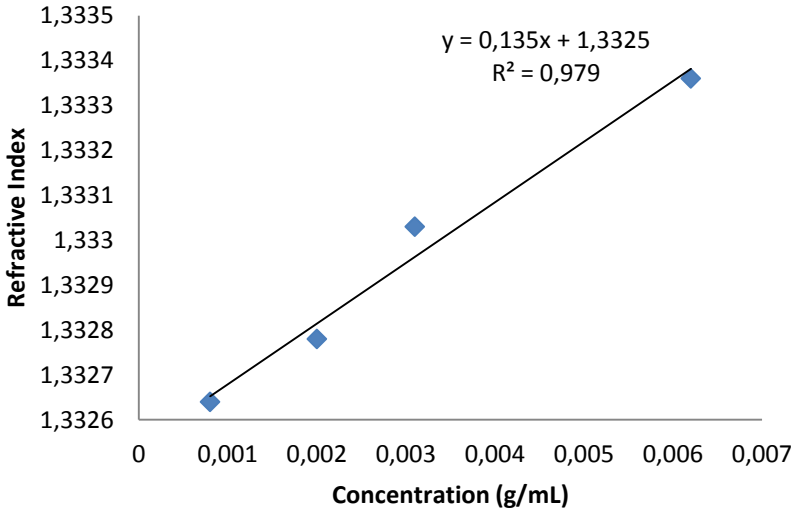

Figure A2 - Determination of the dn/dc parameter to the surfactant Amber 4001.

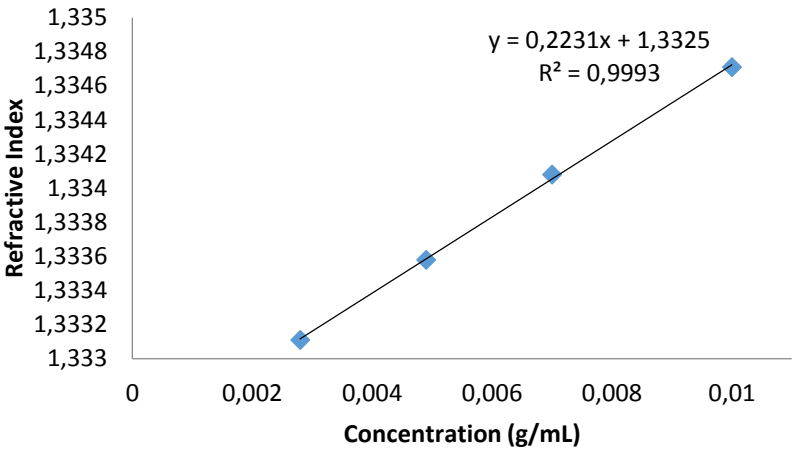

Figure A3 - Determination of the dn/dc parameter to the surfactant Disperse 31.

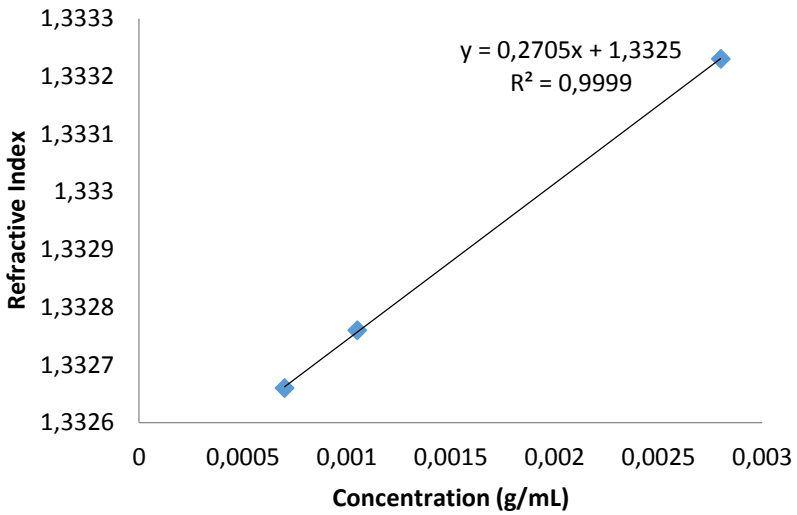

Figure A4 - Determination of the dn/dc parameter to the surfactant Disperse 32.

Appendix B

Size distributions by intensity of the surfactants

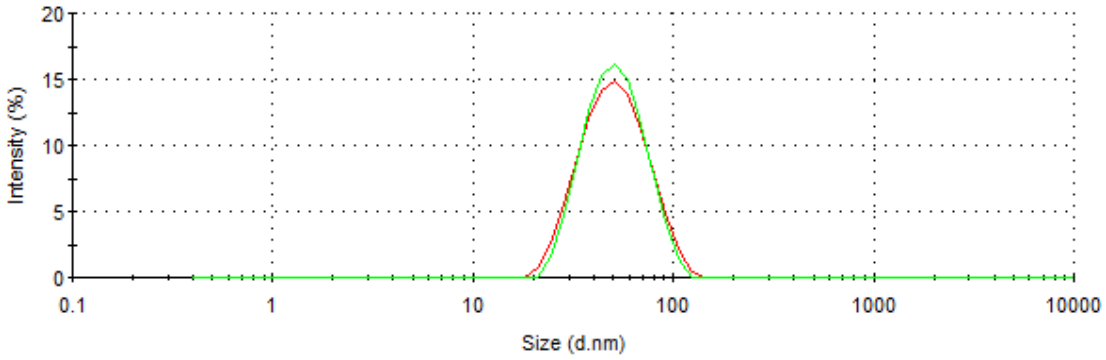

Figure B1- Size distributions by intensity of the surfactant Glycerox.

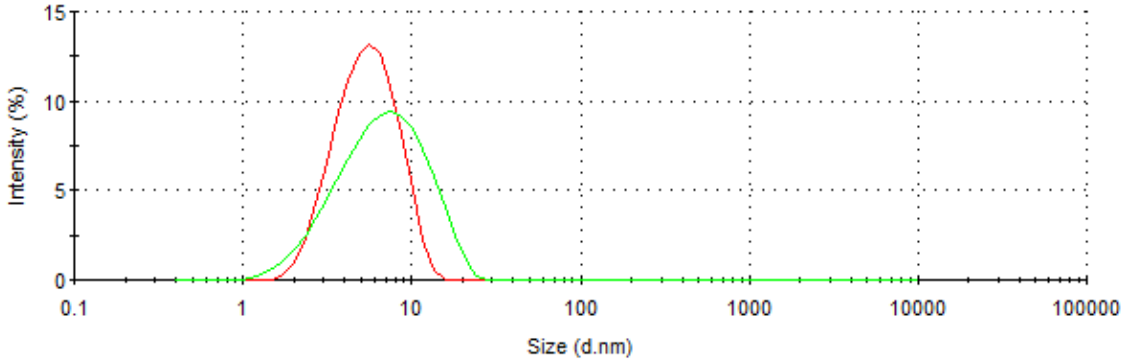

Figure B2 - Size distributions by intensity of the surfactant Amber 4001.

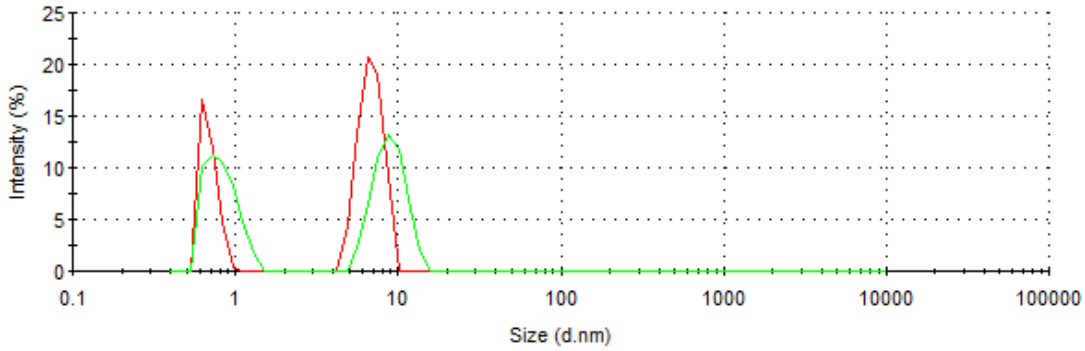

Figure B3- Size distributions by intensity of the surfactant Disperse 31.

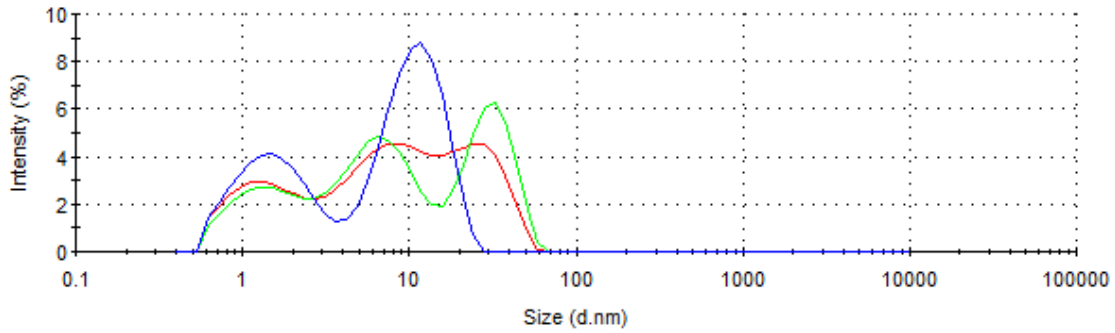

Figure B4- Size distributions by intensity of the surfactant Disperse 32.

Appendix C

Debye Plots

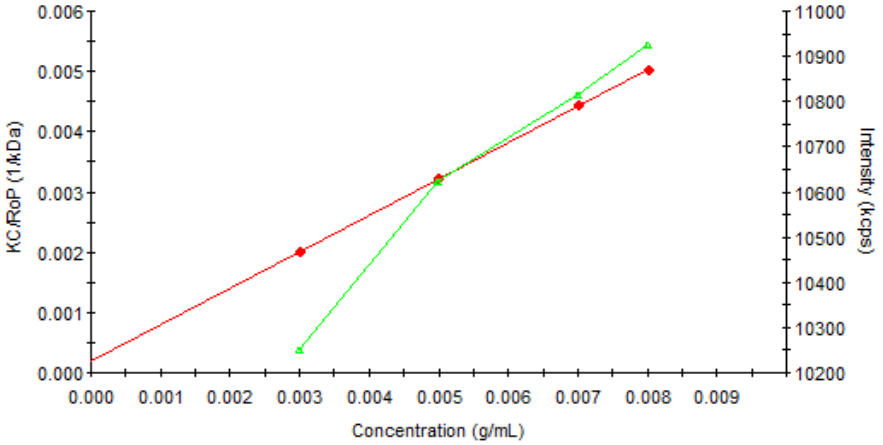

Figure C1- Debye plot used for molecular weight determination of surfactant Glycerox.

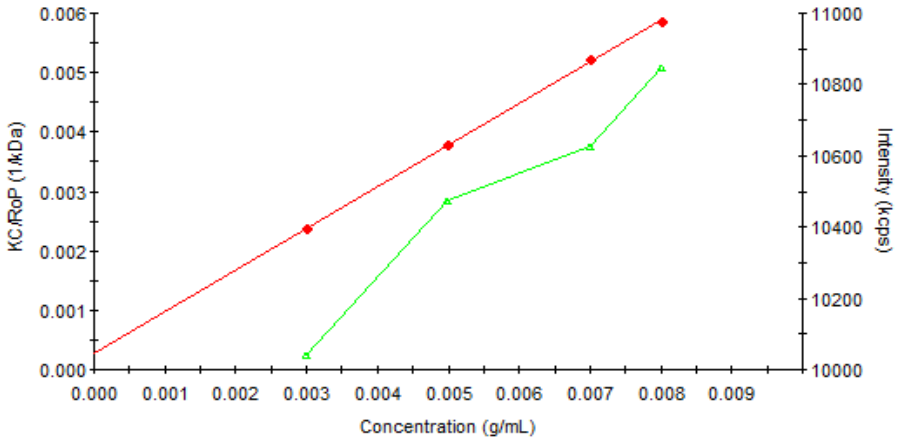

Figure C2- Debye plot used for molecular weight determination of surfactant Glycerox.

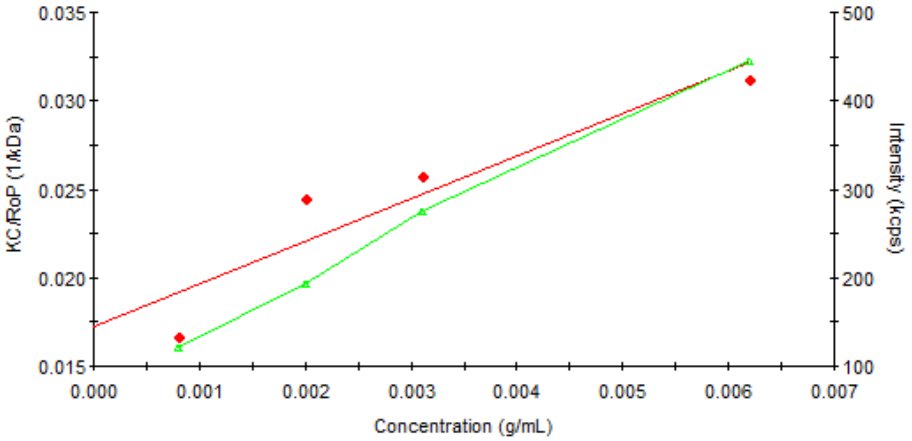

Figure C3- Debye plot used for molecular weight determination of surfactant Amber 4001.

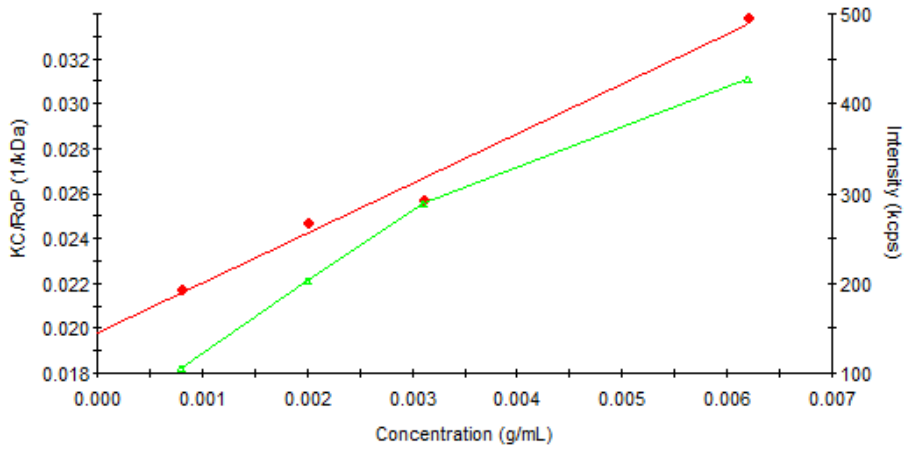

Figure C4- Debye plot used for molecular weight determination of surfactant Amber 4001.

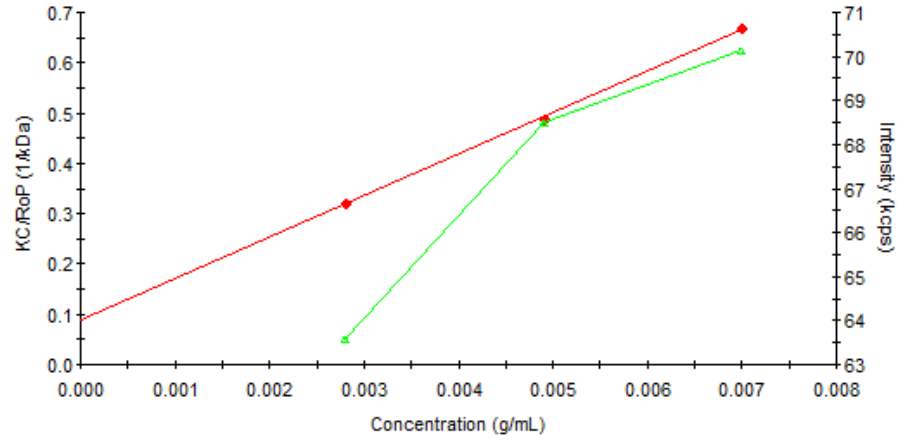

Figure C5- Debye plot used for molecular weight determination of surfactant Disperse 31.

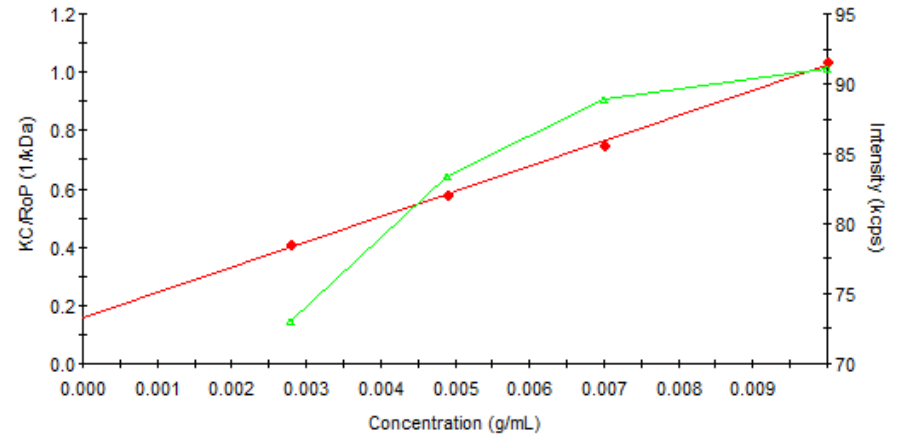

Figure C6- Debye plot used for molecular weight determination of surfactant Disperse 31.

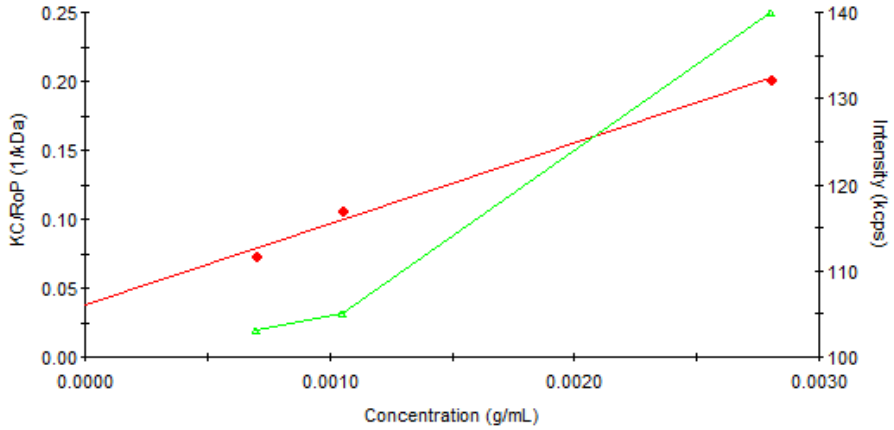

Figure C7- Debye plot used for molecular weight determination of surfactant Disperse 32.

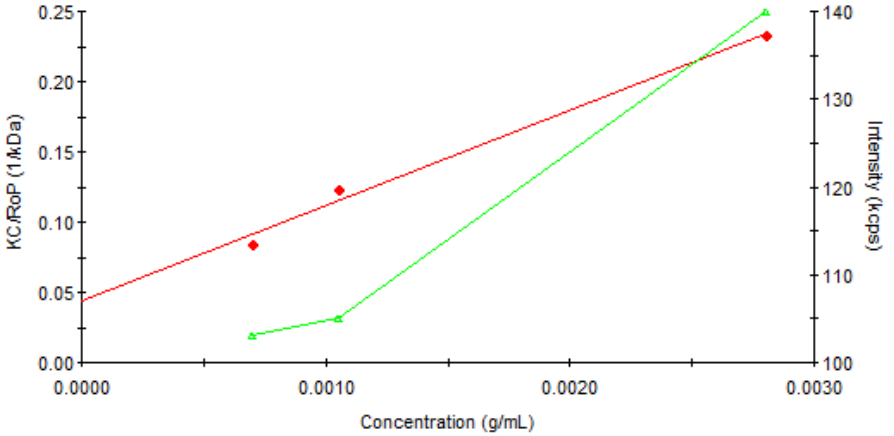

Figure C8- Debye plot used for molecular weight determination of surfactant Disperse 32.

Appendix D

Dispersions of 0.01% of MWCNT in Glycerox and Amber 4001

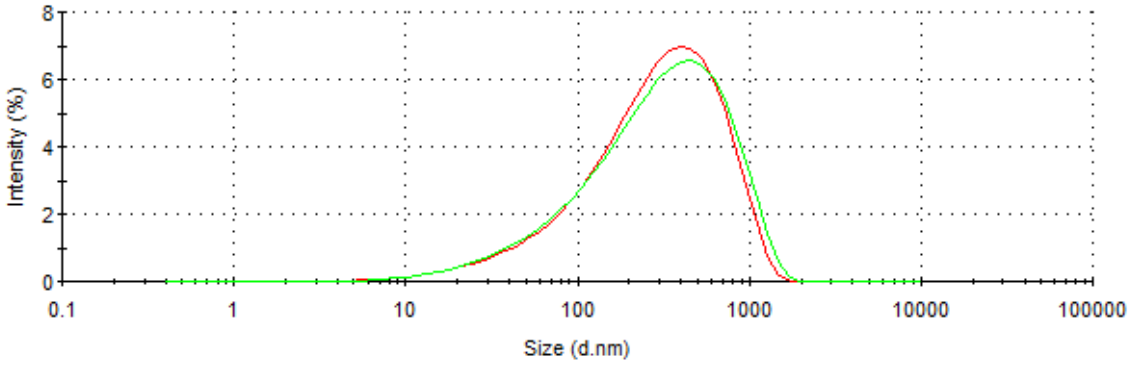

Figure D1- Size distributions by intensity for MWCNT dispersion in aqueous solution enriched with the surfactant Glycerox at 0.5%.

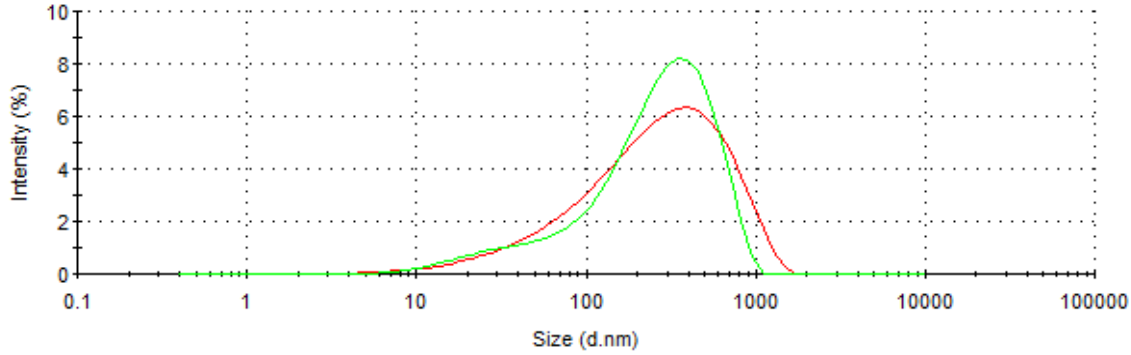

Figure D2- Size distributions by intensity for MWCNT dispersion in aqueous solution enriched with the surfactant Glycerox at 1%.

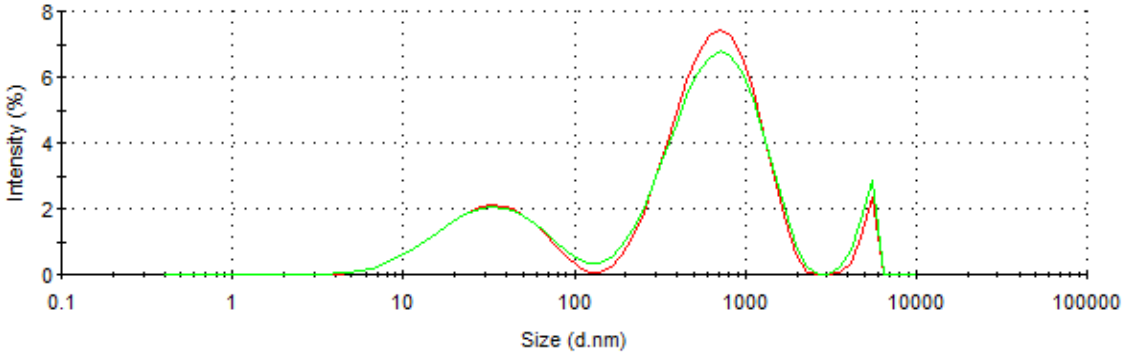

Figure D3- Sizes distributions by intensity for MWCNT dispersion in aqueous solution enriched with the surfactant Glycerox at 3%.

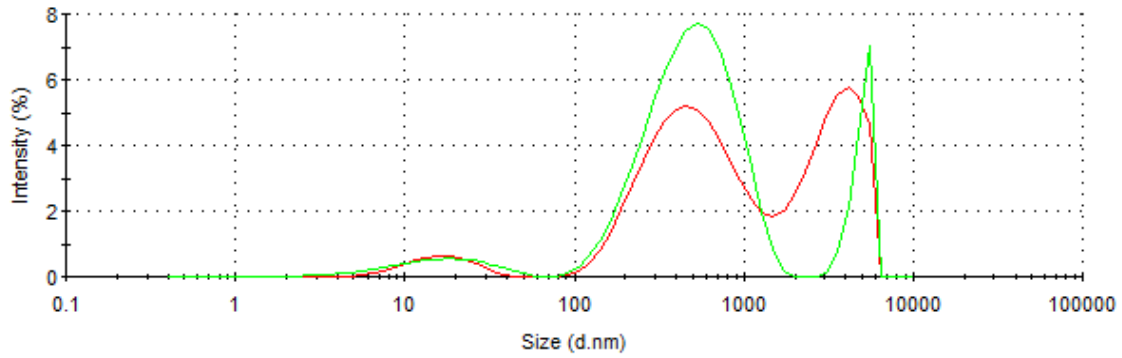

Figure D4- Size distributions by intensity for MWCNT dispersion in aqueous solution enriched with the surfactant Amber 4001 at 0.5%.

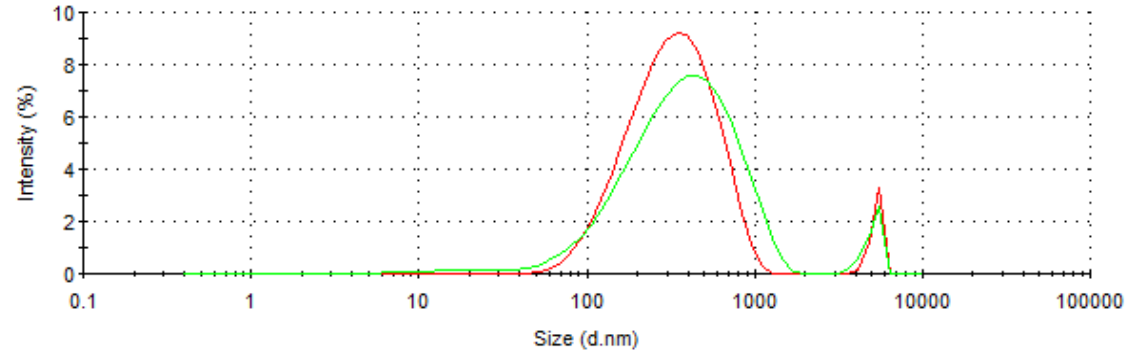

Figure D5- Size distributions by intensity for MWCNT dispersion in aqueous solution enriched with the surfactant Amber 4001 at 1%.

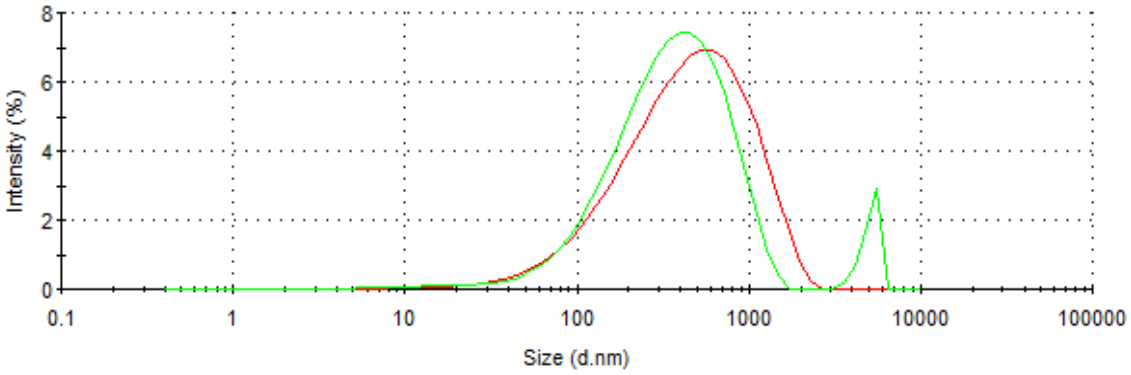

Figure D6- Size distributions by intensity for MWCNT dispersion in aqueous solution enriched with the surfactant Amber 4001 at 3%.